Available online at www.sciencedirect.com

ScienceDirect

Geochimica et Cosmochimica Acta 138 (2014) 57–80

Geochimica et Cosmochimica Acta

www.elsevier.com/locate/gca

Discerning the timing and cause of historical mortality events in modern *Porites* from the Great Barrier Reef

Tara R. Clark [a,*], Jian-xin Zhao [a,*], George Roff [b], Yue-xing Feng [a], Terence J. Done [c], Luke D. Nothdurft [d], John M. Pandolfi [e]

[a] *Radiogenic Isotope Facility, School of Earth Sciences, The University of Queensland, Brisbane, QLD 4072, Australia*
[b] *School of Biological Sciences, The University of Queensland, Brisbane, QLD 4072, Australia*
[c] *Australian Institute of Marine Science, Townsville, QLD 4810, Australia*
[d] *Earth, Environmental and Biological Sciences, Queensland University of Technology, Brisbane, QLD 4000, Australia*
[e] *Centre for Marine Science, Australian Research Council Centre of Excellence for Coral Reef Studies, School of Biological Sciences, The University of Queensland, Brisbane, QLD 4072, Australia*

Received 11 March 2013; accepted in revised form 16 April 2014; available online 28 April 2014

Abstract

The life history strategies of massive *Porites* corals make them a valuable resource not only as key providers of reef structure, but also as recorders of past environmental change. Yet recent documented evidence of an unprecedented increase in the frequency of mortality in *Porites* warrants investigation into the history of mortality and associated drivers. To achieve this, both an accurate chronology and an understanding of the life history strategies of *Porites* are necessary. Sixty-two individual Uranium–Thorium (U–Th) dates from 50 dead massive *Porites* colonies from the central inshore region of the Great Barrier Reef (GBR) revealed the timing of mortality to have occurred predominantly over two main periods from 1989.2 ± 4.1 to 2001.4 ± 4.1, and from 2006.4 ± 1.8 to 2008.4 ± 2.2 A.D., with a small number of colonies dating earlier. Overall, the peak ages of mortality are significantly correlated with maximum sea-surface temperature anomalies. Despite potential sampling bias, the frequency of mortality increased dramatically post-1980. These observations are similar to the results reported for the Southern South China Sea. High resolution measurements of Sr/Ca and Mg/Ca obtained from a well preserved sample that died in 1994.6 ± 2.3 revealed that the time of death occurred at the peak of sea surface temperatures (SST) during the austral summer. In contrast, Sr/Ca and Mg/Ca analysis in two colonies dated to 2006.9 ± 3.0 and 2008.3 ± 2.0, suggest that both died after the austral winter. An increase in Sr/Ca ratios and the presence of low Mg-calcite cements (as determined by SEM and elemental ratio analysis) in one of the colonies was attributed to stressful conditions that may have persisted for some time prior to mortality. For both colonies, however, the timing of mortality coincides with the 4th and 6th largest flood events reported for the Burdekin River in the past 60 years, implying that factors associated with terrestrial runoff may have been responsible for mortality. Our results show that a combination of U–Th and elemental ratio geochemistry can potentially be used to precisely and accurately determine the timing and season of mortality in modern massive *Porites* corals. For reefs where long-term monitoring data are absent, the ability to reconstruct historical events in coral communities may prove useful to reef managers by providing some baseline knowledge on disturbance history and associated drivers.

1. INTRODUCTION

There is a general consensus that coral reefs appear to be declining on a global scale (Hughes et al., 2003; Pandolfi

* Corresponding authors. Tel.: +61 7 6643 9755; fax: +61 7 3365 8530.
E-mail addresses: t.clark1@uq.edu.au (T.R. Clark), j.zhao@uq.edu.au (J.-x. Zhao).

http://dx.doi.org/10.1016/j.gca.2014.04.022
0016-7037/

et al., 2003; Bellwood et al., 2004; Wilkinson, 2008), with the seriousness of this decline manifested in the unprecedented increase in the frequency of mortality in massive corals (Mumby et al., 2001; Carilli et al., 2010; Yu et al., 2012a,b). According to previous studies and quantitative assessments of mortality, slower growing species from the genus *Porites* are considered to be more resistant to bleaching and other environmental perturbations compared to fast growing, ephemeral species such as *Acropora* (Done, 1987; Wesseling et al., 1999; Done et al., 2007). Yet the past century has seen an increase in the number of reports of broad scale, whole colony mortality in corals more than 200 years old, which is cause for worldwide concern (Mumby et al., 2001; Suzuki et al., 2003; Yu et al., 2006, 2012a,b). Many of these events have been linked to El Niño induced warming of sea surface temperatures (Glynn, 1983; Baird and Marshall, 1998; Yu et al., 2006, 2012a,b) and crown-of-thorns starfish (COTS) outbreaks (Done, 1987, 1988; DeVantier and Done, 2007). Therefore, whole or partial mortality in massive *Porites* colonies can provide a means for understanding the frequency and timing of disturbance events both for this species and adjacent coral communities (Done, 1987; Yu et al., 2010).

Porites corals are of ecological significance because they create three-dimensional habitats for fishes and other organisms and contribute to reef growth as either primary or secondary framework builders (Endean and Cameron, 1985; Done and Potts, 1992; van Woesik and Done, 1997). Thus, an understanding of disturbance history in massive *Porites* is important for understanding the impact of current events as well as to predict the future response of this genus to environmental disturbances (Hendy et al., 2003a). This is of major concern as current predictions suggest an increased rate of mortality with increasing anthropogenic disturbance and climate change (Wakeford et al., 2008; Thompson and Dolman, 2010; Pandolfi et al., 2011).

On the Great Barrier Reef (GBR), reports of historical mortality in massive *Porites* are mostly limited to the past ~50 years following the first accounts of catastrophic *Acanthaster planci*, commonly known as crown-of-thorns starfish (COTS), outbreaks in the 1960's (Done, 1992), with few extending beyond this time period (e.g. Hendy et al., 2003b). Moreover, the Australian Institute of Marine Science (AIMS) long-term monitoring program which began in 1986, currently surveys only ~47 out of ~2900 (~1.6%) reefs on the GBR (Sweatman et al., 2011). Therefore little is known about the history of mortality in massive *Porites* including the frequency of mortality and rates of recovery over broad spatial and temporal scales.

Growth discontinuities (or hiatuses) and visible changes in the coral skeleton provide a valuable archive for understanding past environmental stresses (Smithers and Woodroffe, 2001; Suzuki et al., 2003; Hendy et al., 2003b; DeVantier and Done, 2007; Nothdurft and Webb, 2009a). However, many of these studies are limited to colonies whose time of death or collection is accurately known and rely on density band counting techniques to place the growth discontinuities in an accurate chronological timeframe. Advanced isotopic dating techniques such as Uranium–Thorium (U–Th) dating can be used to reconstruct historical mortality events in dead massive coral colonies of unknown age, linking them with major disturbances such as El Niño and storm activity (Yu et al., 2006, 2012a,b).

For inshore reef coral communities, identifying the potential cause for coral mortality can be confounded by a synergy of two or more factors. For example, local stressors such as poor water quality can reduce the thermal tolerance of a coral to be able to withstand abrupt disturbances such as bleaching (Carilli et al., 2010). Alternatively, a severe bleaching or flood event may be followed in quick succession by another disturbance, such as a disease outbreak, with the latter responsible for mortality (e.g. Whelan et al., 2007). Many coral assemblages are also impacted by multiple disturbances over a short period of time (<3 years) (Hughes and Jackson, 1985; Done et al., 2007), which then makes it difficult to identify the primary cause of mortality when the limit of precision for U–Th dating is ± 1–5 years at best.

A further confounding factor that can interfere with precise age dating of mortality is the presence of initial and/or detrital 230-thorium ($^{230}Th_0$) in young (<500-year old) coral skeletons. For a sample to be reliably dated, all of the ^{230}Th in the coral must be produced from the radioactive decay of its parent nuclide ^{234}U, which itself is a daughter product of ^{238}U decay. However, this requisite is often violated with the uptake of various forms of $^{230}Th_0$ by the coral during skeletogenesis. Because the amount of ^{230}Th produced by *in situ* decay is extremely small in young coral samples (e.g. ~660 times less in a 100-year old coral compared to a ~100,000-year old colony), the presence of even small amounts of $^{230}Th_0$ can cause the U–Th age to be significantly older than the true age of the sample (for review see Zhao et al., 2009). The correction for $^{230}Th_0$ can also introduce significant age error, making the corrected ages less useful or even meaningless in addressing ecological questions and trying to link mortality with specific events. In coastal environments, the primary source of $^{230}Th_0$ is from terrestrially derived particulates such as silts and clays (Shen et al., 2008). In order to achieve both accurate and precise U–Th ages, attempts must be made to either actively remove the $^{230}Th_0$ component in the coral skeleton using vigorous cleaning procedures, or correct for the presence of the $^{230}Th_0$ using a well constrained $^{230}Th/^{232}Th_0$ value (Cobb et al., 2003; Yu et al., 2006; Shen et al., 2008; Clark et al., 2012).

Combining both isotopic dating and trace element analysis has proven to be successful in precisely dating and characterising the timing of historical mortality events and the duration of growth hiatuses in *Porites* corals of Holocene age (Yu et al., 2004, 2010). While skeletal Sr/Ca ratios are generally used as a proxy for the reconstruction of sea surface temperatures (Beck et al., 1992; McCulloch et al., 1994; Gagan et al., 2000), they have also been used to identify the season of mortality and any thermal anomalies that may have coincided with mortality in massive *Porites* colonies (Hendy et al., 2003a; Yu et al., 2010). Moreover, a combination of high resolution proxy measurements for SST (such as Sr/Ca), salinity ($\delta^{18}O$) and biological activity ($\delta^{14}C$, Mn and rare earth element

concentrations) recorded in massive *Porites* skeletons, was used to link the 1997 catastrophic death of the Mentawai Islands reef ecosystem, Indonesia, to anomalous Indian Ocean Dipole upwelling and giant red tide (Abram et al., 2003). Combining the techniques used in these studies provides an opportunity to date and understand potential drivers of historical mortality events for both inshore reef *Porites* and adjacent coral communities from the GBR.

In this paper, we assess the applicability of Uranium–Thorium (U–Th) dating and trace element analysis, in conjunction with the examination of coral skeletal mineralogy and texture using scanning electron microscopy to reconstruct the timing and potential causes of recent mortality events in 50 massive *Porites* colonies from the inshore, central GBR. Using high-pressure cleaning to remove detrital Th as well as sample-specific initial $^{230}Th/^{232}Th$ values for initial ^{230}Th correction (Clark et al., 2012, submitted for publication; Roff et al., 2013), we attempt to improve the precision and accuracy of the ^{230}Th ages obtained using U–Th dating methods in order to identify periods of disturbance from several reefs within the Palm Islands region. Monthly resolution Sr/Ca, Mg/Ca and Ba/Ca measurements are also employed to further refine the timing of mortality in a sub-sample of colonies.

2. MATERIALS AND METHODS

2.1. Regional setting

Numerous large *Porites* colonies are common on the leeward side of many of the inshore platform and fringing reefs of the Palm Islands (18°30′–19°00′S and 146°25′–146°45′E) situated 20–40 km offshore in the central GBR (Fig. 1). This region is routinely exposed to sediment laden flood plumes from the Burdekin River (130 km south-east), Herbert River (25 km to the north) and several smaller local rivers. Sediment influx to this region is estimated to have increased five to tenfold since European settlement (McCulloch et al., 2003) as a result of extensive clearing of adjacent catchment areas for cattle grazing (Furnas, 2003; McCulloch et al., 2003). However, the re-suspension of fine sediments is believed to be primarily responsible for the constantly turbid conditions (Larcombe and Woolfe, 1999). Disturbances such as cyclones and bleaching have also been frequent over the past 30 years and are reported to have impacted local coral communities to some degree (Supplementary Table S1).

2.2. Sample collection and preparation

In May 2008 and August 2009, 50 *Porites* colonies suffering more than 50% mortality were sampled from the leeward side of Pandora Reef, Havannah and Pelorus Island (Table 1; Figs. 1 and 2). This area of the reef is generally a low energy or protected environment that greatly increases the fidelity of death assemblage remains for historical analysis by reducing the risk of transportation and breakage (Pandolfi and Greenstein, 1997; Ferguson, 2008). Both spherical and lobed colonies [characteristic of colonies that have experienced past upper surface mortality and regrowth from surviving polyps (Hendy et al., 2003a,b)] were sampled, although smaller colonies ⩽30 cm were avoided as mortality could have resulted from multiple interacting factors [e.g. overgrowth by faster growing corals and sediment accumulation caused by the re-suspension of bottom waters (Done and Potts, 1992)]. Of the colonies investigated in this study, 30% showed clear preservation of corallite structure at the surface of the colony (Fig. 5), suggesting that external bio-erosion was minimal, and the surface age of the colony would accurately represent the time of mortality. For those that did not, the surface age provided the maximum age at the time of mortality, given that the latest stages of growth could have been eroded away.

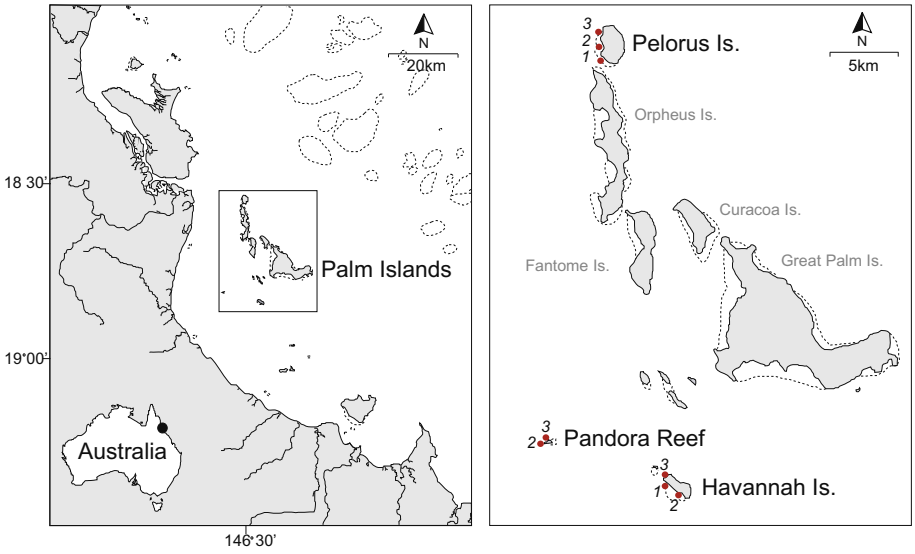

Fig. 1. Location of the Palm Islands, central inshore GBR (left). Enlargement of the Palm Islands region (right). Near spherical *Porites* colonies suffering close to 100% mortality were sampled from Pelorus Island, Havannah Island and Pandora Reef. Numbers 1, 2 and 3 correspond to site locations.

Table 1
Co-ordinates and collection dates for dead *Porites* colonies sampled from the Palm Islands region, central GBR, at Pelorus Island, Havannah Island and Pandora Reef.

Sample name	Lat	Long	No. colonies sampled	Collection dates
Pelorus Island				
Site 1 (PelS1)	18°32′37″	146°29′19″	3	Aug 2009
Site 2 (PelS2)	18°33′15″	146°29′18″	5	May 2008, Aug 2009
Site 3 (PelS3)	18°33′39″	146°29′25″	5	May 2008, Aug 2009
Havannah Island				
Site 1 (HavS1)	18°50′25″	146°32′01″	13	May 2008, Aug 2009
Site 2 (HavS2)	18°50′38″	146°32′13″	3	May 2008, Aug 2009
Site 3 (HavS3)	18°50′01″	146°31′58″	6	Aug 2009
Pandora Reef				
Site 2 (PanS2)	18°48′54″	146°25′38″	2	Aug 2009
Site 3 (PanS3)	18°48′46″	146°25′37″	13	May 2008, Aug 2009

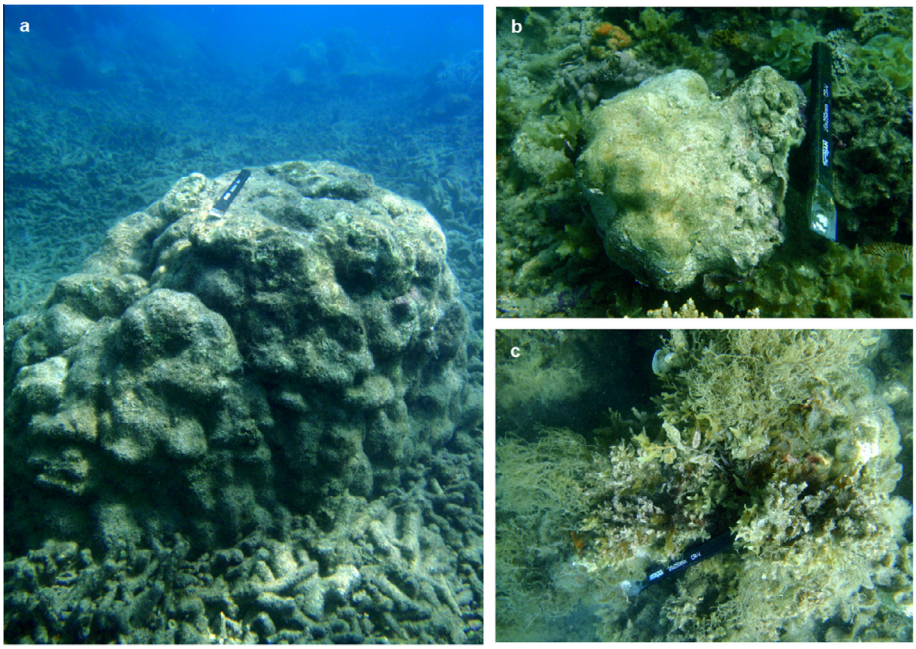

Fig. 2. Images of *in situ* dead *Porites* sampled in this study; (a) Dead *Porites* from Pelorus Island surrounded by dead *Acropora* rubble substrate; (b) Transported dead *Porites* from Havannah Island; (c) Dead *Porites* concealed by macroalgae at Havannah Island. Chisel is approximately 30 cm in length.

Samples of dead coral skeleton ~6 cm in length were removed using a hammer and chisel on SCUBA at depths ranging between 2–3 m. Each sample was cut along the main growth axis into a 7 mm section, photographed and X-rayed to produce an image of annual density banding patterns.

The photograph of each sample was analysed using Image J (Abramoff et al., 2004) to provide a coarse quantitative, unbiased measure of the preservation state of the sample. After setting the scale in the image, an outline of the sample was drawn to calculate the total area (in cm^2). An automated function was then used to convert the image to binary, or threshold the image, to include only the darker (bioeroded, discoloured) areas of the sample. An outline of each of these altered regions was drawn and the area calculated (in cm^2). The combined total was then used to calculate the proportion of the area altered with respect to the total area of the sample. This was cross-checked by visually assessing the sample.

Using the X-ray as a guide, approximately 1–2 g of skeleton was then removed from within an easily identifiable band in areas of the colony section that was free from discolouration and evidence of bioeroding organisms using a clean bench drill with a bit size of 0.5 cm. Table 4 lists the number of growth bands above the sampling location that is required to be added to the ^{230}Th age to estimate the time of mortality. The majority of samples were crushed using an agate mortar and pestle to an approximately 1 mm size fraction and centrifuged with 10% H_2O_2 to remove organics. The remaining samples were kept as whole. All samples were then ultrasonically cleaned in Milli-Q water 3–4 times until no visible contaminants were evident and

dried on a hotplate at 40 °C (Shen et al., 2008). Only the cleanest fragments free from discolouration and any visible forms of alteration were selected from under a microscope and used for U–Th dating.

2.3. U–Th dating

2.3.1. Sample digestion, spiking and U–Th column chemistry procedures

A total of 62 samples were taken from 50 colonies (including replicate analyses on the following colonies: PelS2C02-09, HavS1C02.1-09, HavS1C05.1-09, HavS1C17.2-08, HavS3C05.1-09, PanS2C02-09, PanS3C02-09, PanS3C11-08, PanS3C12-08 and PanS3C15-08), and prepared for U–Th dating at the Radiogenic Isotope Facility (RIF), the University of Queensland, following column chemistry procedures similar to that described by Zhao et al. (2001) and Clark et al. (2012). The samples were dated initially by a WARP-filtered high-abundance-sensitivity VG Sector-54 thermal ionization mass spectrometer (TIMS) and then by a Nu Plasma multi-collector inductively coupled plasma mass-spectrometer (MC-ICP-MS) (since its installation in April 2010) at the Radiogenic Isotope Facility, The University of Queensland, over a period of 5 years. For TIMS analysis, approximately 1 g of each sample was spiked with a ^{229}Th–^{233}U–^{236}U mixed tracer. For MC-ICP-MS, samples varying between 1.0–0.3 g in size were spiked with a ^{229}Th–^{233}U mixed tracer. After complete digestion in double-distilled nitric acid, the sample beakers were then tightly capped and placed overnight on a hot-plate at 90 °C to allow for complete homogenisation of the tracer-sample mixed solution. Sample solutions were then allowed to dry on a hot-plate and U and Th were pre-concentrated by co-precipitation with $Fe(OH)_3$. The hydroxide precipitates were then redissolved in 7N HNO_3 and purified using standard ion-exchange methods (Edwards et al., 1987).

2.3.2. TIMS and MC-ICP-MS analytical protocol

For TIMS analysis, the U and Th fractions of fifteen samples were loaded separately onto single filaments made of zone-refined rhenium ribbons between two graphite layers. The filaments were then loaded into the TIMS, with the U isotopes measured fully-automatically during the night and the Th isotopes measured manually during the day following the protocol described in detail by Clark et al. (2012).

For MC-ICP-MS analysis, the U and Th separates for the rest of the samples were re-mixed in 2% HNO_3 to make ~3 ml solution in a pre-cleaned 3.5 ml test tube. The mixed solution for each sample contains the entire Th fraction and a small percentage of the U fraction. The amount of U fraction to be added to the mixed solution was calculated based on the U concentration in the coral, column recovery rate for U, and the MC-ICP-MS working sensitivity, aiming to achieve 3–5 volts of ^{238}U signal. The tubes containing the 3 ml solution were then centrifuged at 4000 rpm for 20 min to draw out any suspended material (mainly any trace amounts of leaked resin from the columns) from the solution to the bottom of the tube to avoid this material being introduced into the MC-ICP-MS.

The U–Th mixed solution was injected into the MC-ICP-MS through a DSN-100 desolvation system with an uptake rate of around 0.12 ml min^{-1}. U–Th isotopic ratio measurement followed a similar analytical protocol previously described by Hellstrom (2003), but with minor modification to the detector configuration as described first in Zhou et al. (2011) e.g. the U–Th isotopes were measured in two sequential cycles with masses 237 and 236 set on the axial Faraday cup (Table 2), instead of three cycles as used by Hellstrom (2003).

Combined use of the two secondary electron multipliers (SEM) and Faraday cups requires the determination of the Faraday cup-SEM relative gain. The relative gain can be derived by alternately measuring a beam of appropriate intensity (e.g. for SEM2 ^{229}Th ~2 mV and SEM0 ^{233}U 10 mV) with the SEMs and Faraday cups in peak jumping (multi-static) mode. This approach is conducted as a two-cycle measurement with ^{229}Th and ^{233}U alternately cycled through the SEMs and Faraday cups (see shaded grey in Table 2). In our protocol, the Faraday–SEM relative gain is determined by normalizing the Faraday–Faraday ^{229}Th/^{233}U measured in cycle 1 to the Faraday–SEM ^{229}Th/^{233}U measured in cycle 2. The measured gains are then used to correct ^{230}Th/^{238}U and ^{229}Th/^{238}U raw ratios. Because the gain is calculated from the ratios, fluctuation of the signal intensity is cancelled.

It is worthwhile to note that the MasCon multipliers installed on our Nu Plasma MC-ICP-MS have superb linearity for signal sizes in the range of 10,000 to 1,000,000 cps (corresponding to ~0.2 mV to 20 mV on the Faraday cup, assuming the SEM gains ~75%), as demonstrated in our repeated measurements of standards and replicates with different signal sizes and different sample:spike ratios. For smaller signals <10,000 cps, unlike the ETP multipliers, the degree of non-linearity on our MasCon multipliers (both SEM0 and SEM2) appear to be below the analytical precision of the measured isotopic ratios. For example, we have spiked our in-house U-metal (CRM-112A) solutions with our ^{229}Th–^{233}U mixed tracer and measured the solutions (~10, ~15 and ~20 ppb) directly on the MC-ICP-MS without column separation. Despite the ^{230}Th signal being only 2–4 cps, our repeated measurements yielded consistent ages within error of 1936 ± 5 A.D. (Table 3), consistent with values reported in McCulloch and Mortimer (2008). In addition, we also spiked a large aliquot with our ^{229}Th–^{233}U mixed tracer and performed column separation of U and Th on the spiked solution. Then we mixed the total Th fraction with a small percentage of the U fraction to achieve signal sizes of ^{238}U ~7 volts and ^{230}Th ~80 cps. Two measurements with different spike types yielded indistinguishable ages of 1935.9 ± 0.7 and 1936.5 ± 0.5 A.D. About <10% of the left-over solutions were then diluted >10 times and re-measured on the MC-ICP-MS with ^{230}Th signals of 7.6 and 5.8 cps, respectively. The resultant ages are 1934.6 ± 2.0 and 1936.7 ± 2.7 A.D., respectively, which is within error of the more precise ages based on larger ^{230}Th signals. These results clearly testify the robustness of our analytical protocols which are free of issues related to multiplier non-linearity, DSN-100 carry-over memory and spike calibration.

Table 2
The Nu Plasma MC-ICP-MS detector configuration used for the analytical protocol in this study.

	Axial Mass	Time/s	L5	SEM2 (filter on)	L4	SEM1 (off)	L3	SEM0 (filter off)	L2	L1	Ax	H1	H2
Baseline*	**236.5**	25	228.5	229.5			232.5	233.5	234.5		236.5	237.5	238.5
Baseline*	**237.5**	25	229.5	230.5			233.5	234.5	235.5		237.5	238.5	239.5
Seq. 1	**236.0**	6(5)†		^{229}Th			^{232}Th	^{233}U		^{235}U			^{238}U
Seq. 2	**237.0**	16(17)†	^{229}Th	^{230}Th			^{233}U	^{234}U	^{235}U			^{238}U	

In this configuration, each sample is measured in three blocks each consisting of 10 cycles (each cycle is composed of two sequences).
Two types of detectors are used in this protocol, including secondary electron multipliers (SEM) and Faraday cups: Secondary electron multipliers (SEM): SEM2, SEM1, SEM0 (SEM1 is disabled), Faraday cups: L5, L4, L3, L2, L1, Ax, H1, H2.
^{229}Th and ^{233}U (in grey shaded cells) are measured on the SEMs and Faraday cups alternatively in both sequences to work out the SEM-Faraday cup relative gains. The measured gains are used to correct ^{230}Th/^{238}U and ^{229}Th/^{238}U raw ratios. The average of measured ^{238}U/^{235}U ratios in both sequences is normalised to 137.82 (Amelin et al., 2010) to work out the bias factor to correct for mass fractionation on other ratios using the exponential law.
* Half-mass baselines are measured for a total of 50 s on both sides of each isotope-peak in Sequence 2 before each block starts. The geometric mean of the baselines measured on each detector is used for baseline extraction from the isotope signals on the respective detector.
† Numbers in parentheses denote time (in seconds) that was used for some samples with very low ^{230}Th signal.

Table 3
MC-ICP-MS data for U-metal (CRM-112A) solutions spiked with a ^{229}Th–^{233}U and ^{233}U–^{236}U–^{229}Th mixed tracer.

Sample name	(^{234}U/^{238}U)	^{230}Th Age (years)	^{230}Th age (A.D.)	^{238}U (volts)	^{230}Th (cps)
U metal/^{233}U–^{229}Th spike#1*	0.9627 ± 0.0007	74.9 ± 0.7	1935.9	7.7	83.4
U metal/^{233}U–^{229}Th spike#1* †	0.9602 ± 0.0007	76.2 ± 2.0	1934.6	6.3	7.6
U metal/^{233}U–^{236}U–^{229}Th spike#1*	0.9605 ± 0.0007	74.2 ± 0.6	1936.6	7.7	81.3
U metal/^{233}U–^{236}U–^{229}Th spike#1* †	0.9612 ± 0.0010	74.1 ± 2.9	1936.7	6.2	5.8
U metal/^{233}U–^{236}U–^{229}Th spike#1	0.9623 ± 0.0008	76.0 ± 3.5	1934.6	4.3	4.6
U metal/^{233}U–^{236}U–^{229}Th spike#1	0.9636 ± 0.0006	73.0 ± 2.6	1937.6	5.8	7.3
U metal/^{233}U–^{236}U–^{229}Th spike#1	0.9634 ± 0.0007	70.2 ± 3.5	1940.4	5.6	2.7
U metal/^{233}U–^{236}U–^{229}Th spike#2	0.9628 ± 0.0008	78.4 ± 4.5	1932.2	6.3	3.2
U metal/^{233}U–^{236}U–^{229}Th spike#2	0.9629 ± 0.0009	72.8 ± 2.8	1937.8	6.3	6.0
U metal/^{233}U–^{236}U–^{229}Th spike#2	0.9618 ± 0.0007	74.8 ± 1.8	1935.8	6.1	9.6
U metal/^{233}U–^{229}Th spike#1	0.9631 ± 0.0006	77.3 ± 3.9	1933.3	4.0	4.3
U metal/^{233}U–^{229}Th spike#1	0.9636 ± 0.0010	71.8 ± 2.9	1938.8	3.9	4.3
U metal/^{233}U–^{229}Th spike#1	0.9630 ± 0.0009	74.1 ± 3.5	1936.5	4.2	4.6
U metal/^{233}U–^{229}Th spike#1	0.9615 ± 0.0007	76.4 ± 3.5	1934.2	4.4	4.8
U metal/^{233}U–^{229}Th spike#1	0.9629 ± 0.0009	72.9 ± 3.3	1937.7	4.4	4.7
U metal/^{233}U–^{229}Th spike#1	0.9621 ± 0.0007	74.2 ± 4.1	1936.4	4.1	4.5
U metal/^{233}U–^{229}Th spike#1	0.9624 ± 0.0009	76.1 ± 4.6	1934.5	3.9	4.4
U metal/^{233}U–^{229}Th spike#1	0.9622 ± 0.0007	71.5 ± 2.7	1939.1	3.8	4.1
U metal/^{233}U–^{229}Th spike#2	0.9643 ± 0.0008	75.4 ± 5.6	1935.4	7.1	3.9
U metal/^{233}U–^{229}Th spike#2	0.9612 ± 0.0006	70.3 ± 6.3	1940.5	7.5	4.0

All errors reported are ± 2σ.
* These data were obtained after column chemistry to pre-concentrate Th. The other samples were measured directly without column chemistry.
† The result was obtained using <10% of the Th fraction separated from the fraction above it, and shows that the age is highly reproducible, regardless of the sample size and spike type.

In addition, the multiplier dead-times have been re-calibrated and new dead-time values calculated, rather than using factory default values for dead-time corrections. This ensures precise measurements of ^{234}U/^{238}U and ^{233}U/^{238}U ratios measured on the SEM0. Dead-time corrections have little influence on ^{229}Th and ^{230}Th signals measured on SEM2, as signal size seldom exceeds 100,000 cps. A deceleration lens behind SEM2 was used to increase the abundance sensitivity by 10 times (compared to unfiltered SEMs), so that the ^{232}Th tailing effect at mass 230 is small enough for accurate correction, regardless of the size of the ^{232}Th/^{230}Th ratio in the sample. The working abundance sensitivity on SEM2 with the filter on is <500 ppb at one mass distance from the large peak in the U–Th mass range, thus the tailing from ^{232}Th on mass 230 is typically <5% of the ^{230}Th peak, even for the least pure coral samples with ^{232}Th/^{230}Th > 100,000. For samples with ^{232}Th/^{230}Th < 10,000, tailing is typically <1%. The tailing contribution was extracted from the ^{230}Th signal by performing simultaneous measurements of baselines at

masses 230.5 and 229.5. The geometric mean of the two half-mass-unit baseline measurements was used in the online acquisition program.

The working sensitivity of our MC-ICP-MS is about 0.4–0.6 volt per ppb for U and 0.35–0.55 volt per ppb of Th at ~0.12 ml min^{-1} uptake rate. Each sample took about 20 min to measure. Prior to a new sample being measured the system was flushed for 15 min with 5% Aqua Regia and then 2% $HNO_3 + 0.03\%$ HF mix to prevent any cross-contamination or 'memory' effect. In the clean-up stage, all isotopes were monitored and raw counts measured on their respective detectors to ensure no carry-over memories from previous samples. Long-term monitoring of carryover memories over 6 months shows that ^{230}Th memory is consistently less than 0.1 ions per second, which is negligible for most samples. The carry-over memory for all other isotopes is also negligible. Measurements of samples, standards, and carryover memories were performed fully automatically using a Cetac ASX-110 auto-sampler (with purpose driven modification).

The 'drift monitor' was made by adding ^{229}Th and ^{233}U spikes separately into a dilute solution of a uranium oxide impurity standard New Brunswick Laboratory-6 (NBL-6) from the USA. The working U concentration in the 'drift monitor' is around 10 ppb, with ^{233}U and ^{229}Th signal sizes typically around 10 and 2 mV, respectively, and its isotopic ratios have been precisely calibrated against the secular equilibrium Harwell Uraninite standard, HU-1 (Stirling et al., 1995; Hellstrom, 2003). In this study the 'drift monitoring' solution was repeatedly measured after every six unknown samples, and the results of this 'drift monitor' were used for monitoring or correcting for long-term drift for a number of parameters such as ion counter gains (if ^{229}Th and/or ^{233}U signals in the samples are too small), and minor bias in the $^{230}Th/^{238}U$ and $^{234}U/^{238}U$ ratios during each session (the bias mainly caused by imperfect signal peak shapes and alignments, as well as uncertainty in the measured SEM dead times). Frequently, measured samples may contain ^{233}U and ^{229}Th that are too low to yield reliable measurements of the Faraday/SEM relative gains. In this instance, gain is calculated by interpolating between two bracketing NBL-6 drift monitors. Long-term monitoring of the SEM gains using the 'drift monitor' shows that the unfiltered SEM0 always drifts downwards by no more than 0.2% over 4 h, whereas the filtered SEM2 often fluctuates by no more than 0.5% over the entire measurement session which can last for several days (due to the much smaller signals applied to this detector resulting in no obvious downward drift during each session). As the SEM2 gain is only used for obtaining the $^{232}Th/^{229}Th$ ratio measurements which are used for initial/detrital ^{230}Th corrections, <0.5% precisions for $^{232}Th/^{229}Th$ are more than sufficient. For mass fractionation corrections, the average of measured $^{238}U/^{235}U$ ratios in both cycles is normalised to 137.82 [this is the most recently assumed ratio between ^{238}U and ^{235}U for USGS standard rocks (Amelin et al., 2010)] to work out the bias factor to correct for instrumental mass fractionation on other ratios using the exponential law (Hart et al., 1989). The natural variability of $^{238}U/^{235}U$ ratios may vary around 0.1% (or up to 0.5%, C. Stirling *pers. comm.*) according to Stirling et al. (2007), Amelin et al. (2010) and others. However, the choice of the normalization value has virtually no influence on the calculated ages of very young samples. This is because the ^{230}Th age is mostly related to the $^{230}Th/^{234}U$ ratio in the sample, with the influence of $^{234}U/^{238}U$ being negligible if the sample is very young. In our laboratory we use a ^{229}Th–^{233}U spike, which means that any mass bias in $^{230}Th/^{229}Th$ measurement is cancelled out by the same degree of mass bias in the $^{234}U/^{233}U$ measurement; thus the measured $^{230}Th/^{234}U$ ratio is independent of the mass fractionation factor used. To demonstrate this, we have performed a test using Isoplot. By adjusting the bias in $^{234}U/^{238}U$ even by 10% (from 1.147 to 1.262), $^{230}Th/^{238}U$ will change by the same percentage so that $^{230}Th/^{234}U$ remains unchanged. The calculated ^{230}Th age for a sample of ~14.3 years old will only change by 1.6 ppm (from 14.318177 to 14.318154); four orders of magnitude smaller than our measured age error.

2.3.3. Procedural and initial ^{230}Th correction

After TIMS and MC-ICP-MS measurements, all U–Th ages were calculated with the Isoplot/Ex 3.00 program (Ludwig, 2003). The total procedural ^{230}Th blank for our MC-ICP-MS U–Th data was determined to be $1.18 \pm 0.24 \times 10^{-10}$ nmol or 0.27 ± 0.05 fg ($N = 10$); contributing an average 0.09 year to the ^{230}Th ages of the samples in this study. The procedural blanks for ^{238}U and ^{232}Th were averaged at $1.4 \pm 0.9 \times 10^{-5}$ nmol (or 3.3 ± 2.2 pg) and $3.0 \pm 1.9 \times 10^{-6}$ nmol (or 0.69 ± 0.41 pg, respectively, which are negligible for coral samples typically containing ~3 ppm U. These values are much lower than the procedural blanks measured using TIMS, where high blank contributions were considered to be a result of more complex column chemistry and the colloidal graphite used to load the sample onto the filaments (Clark et al., 2012). The TIMS ^{230}Th procedural blank correction contributes an average 0.5 year to the ^{230}Th ages of the samples in this study (the larger samples sizes of the TIMS analyses offset the impact of blank corrections on the ages). Procedural ^{230}Th and ^{232}Th blanks for both the MC-ICP-MS and TIMS measurements were extracted from the samples in the Microsoft Excel spreadsheet used for U–Th age calculation.

The presence of initial ^{230}Th was corrected using a model value based on a two-component mixing equation:

$$\left(\frac{^{230}Th}{^{232}Th}\right)_{mix} = \left(\left(\frac{^{232}Th_{live}}{^{232}Th_{dead}}\right) \times \left(\frac{^{230}Th}{^{232}Th}\right)_{live}\right) + \left(\left(\frac{^{232}Th_{dead} - ^{232}Th_{live}}{^{232}Th_{dead}}\right) \times \left(\frac{^{230}Th}{^{232}Th}\right)_{sed}\right)$$

where $^{232}Th_{dead}$ is the measured ^{232}Th value (ppb) in the individual dead coral sample. $^{232}Th_{live}$ is the mean ^{232}Th value (ppb) measured in live *Porites* coral samples collected from the region. Based on seven samples collected from Pandora Reef and neighbouring Pelorus Island, this was determined to be 0.95 ppb. $^{230}Th/^{232}Th_{live}$ represents or approximates the isotopic composition of the hydrogenous component in the dead coral skeleton with an unweighted (conservative) mean atomic ratio of $5.85 \times 10^{-6} \pm 20\%$ (which corresponds to an activity ratio of $1.08 \pm 20\%$).

$^{230}Th/^{232}Th_{sed}$ is the detrital component represented by a weighted mean atomic ratio of $3.30 \pm 0.11 \times 10^{-6}$ [activity ratio of 0.61 ± 0.02 (2σ)], determined from isochron-inferred $^{230}Th/^{232}Th$ ratios obtained from local dead *Porites* coral skeletons (Clark et al., submitted for publication). This value is within error of a mean atomic ratio of $3.51 \times 10^{-6} \pm 20\%$ (which corresponds to an activity ratio of $0.65 \pm 20\%$) derived from 44 ICP-MS analyses of sediments collected from the Burdekin River catchment area (unpublished data from Cooper et al., 2006).

The time of mortality or 'surface age' was calculated by adding the number of growth bands above the sampling location to the U–Th age (Yu et al., 2006). Kernel Density Estimator (KDE) values derived from the surface ages were created using the statistical program R version 3.0.2 (R Core Team, 2013) and the Java-based Density Plotter program (Vermeesch, 2012).

2.4. Trace element analysis

Three *Porites* samples that showed intact corallite structure at the surface of the colony were sampled at a monthly, and in some cases fortnightly, resolution of 12–26 samples per year, respectively, along the main growth axis to determine the season of mortality by measuring Sr/Ca and Mg/Ca ratios using inductively coupled plasma mass spectrometry (ICP-MS). Prior to sampling, each section was soaked in 10% H_2O_2 for 24 h to oxidise any organic material, ultrasonically cleaned in Milli-Q water and dried in an oven at 40 °C (Marshall and McCulloch, 2002; Yu et al., 2010). Using the coral X-rays as a reference, approximately 500 μg of sample was taken at 1 mm increments using a hand held drill and diamond drill bits along the main growth axis. Each bit was ultrasonically cleaned in Milli-Q water and dried under highly pressurised air to prevent cross contamination. This was repeated to cover a time period between 4–6 years of growth in each sample.

All sample preparation was performed under ultra-clean conditions in the Radiogenic Isotope Laboratory, University of Queensland. All labware including ICP-MS tubes were cleaned following a four step cleaning procedure which involved alternately soaking overnight in 10% hydrochloric acid (HCl), 5% double distilled HNO_3 and Milli-Q water at 60 °C. Tubes were then carefully rinsed with Milli-Q water three times and allowed to dry in a fume hood.

Approximately 200 μg of powdered coral sample was then transferred to a pre-cleaned 12 ml polystyrene (PS) tube and dissolved in a 1% HNO_3 stock standard solution containing scandium (Sc), vanadium (V) and yttrium (Y) and made up to 10 ml to achieve a dilution factor of ~1:50,000 times. A calibration standard was made by dissolving 0.02 g of the international reference material Jcp-1, a *Porites* sp. coral issued by the Geological Society of Japan (Okai et al., 2002; Inoue et al., 2004), in 900 ml of 1% standard stock solution. An external monitor solution was also prepared in a similar manner using a *Porites lutea* coral collected from Nha Trang Bay, Vietnam, western South China Sea, which has been routinely measured in the laboratory. A series of blank solutions were also prepared using the standard stock solution. All sample, monitor and calibration solutions were sonicated for 30 min to allow for complete homogenisation prior to analysis.

Both Sr/Ca and Mg/Ca ratios in 215 samples were measured using a Thermo X-Series quadruple ICP-MS at the Radiogenic Isotope Laboratory, the University of Queensland. All measurements were performed within 24 h after carbonates were dissolved in 1% HNO_3 to avoid Mg and Ba contamination leached from the plastic vials (Shen et al., 2007). The internal standard's isotopic signals were used for instant correction of drift in mass response. The calibration standard, external monitor and blank solutions were monitored at regular intervals to assess the reproducibility and correct for long-term instrumental drift during measurement. As Ca is semi-constant in the coral samples, only element/Ca ratios were determined. Therefore precise sample weights were not needed. The Jcp-1 standard solution was measured in between every five samples. The signals of the internal standards ^{45}Sc, ^{51}V and ^{89}Y were used for instant drift correction in mass response, which mainly resulted from matrix difference and instrumental parameters. Repeated measurements of Sr/Ca, Mg/Ca and Ba/Ca ratios in the Jcp-1 standard were used to correct for long-term drift. The recommended Sr/Ca, Mg/Ca and Ba/Ca values for Jcp-1 from the literature (Okai et al., 2002) were used for converting the signal ratios of the samples into mmol/mol ratios. Using previously defined Sr/Ca–SST calibrations for *P. lutea* colonies from the Palm Islands region, Sr/Ca ratios obtained in this study were converted to SSTs using the equation $T = 167.9 - [15{,}649\ (Sr/Ca)_{atomic}]$ (McCulloch et al., 1994; Gagan et al., 1998) in order to provide further information on climatic conditions prior to mortality. Reconstructed SSTs were compared with *in situ* monthly average data obtained from temperature loggers positioned at 6.4 m depth on the reef slope of Havannah Island (AIMS, 2014).

2.5. Scanning electron microscope analysis

In the colonies HavS3C02, HavS3C03 and HavS3C06, a portion ~2 cm in length close to the surface of the colony was cut along the longitudinal axis from the same area where samples were taken for trace-element analysis, embedded in resin, polished, etched in dilute formic acid (2%) for 20 s and coated with gold (Nothdurft et al., 2007). The sample was then inspected under a FEI Quanta 200 environmental scanning electron microscope at the Queensland University of Technology (QUT) for signs of diagenic alteration. Images were taken under high vacuum mode (15 kV) using both secondary and backscattered electron imaging.

2.6. Statistical analysis

To demonstrate that our method was unbiased towards sampling pristine material, and hence colonies of a younger age, Pearson correlation was applied to determine any relationship between sample preservation (using per cent area altered) and ^{230}Th age.

Mortality 'events' were defined as outliers in the ^{230}Th age distribution where KDE values fell beyond the upper extreme values of the box plot (Frigge et al., 1989; Hodge and Austin, 2004). The upper limit (or upper fence) is defined as Q3 + 1.5 (IQR), where Q3 is the upper quartile or 75th percentile and IQR is the inter quartile range [upper quartile (Q3) − lower quartile (Q1)].

KDE values were summed for each year and compared with long-term instrumental or proxy environmental time-series available for the region [such as Burdekin River discharge, sea surface temperature (SST), Pacific Decadal Oscillation (PDO) and El Nino Southern Oscillation (ENSO)] using Pearson correlation. P-values < 0.05 were deemed significant.

3. RESULTS

3.1. U–Th data

The dead *Porites* samples were analysed using TIMS in 2009, and later using MC-ICP-MS in 2010 and 2013. All ^{230}Th ages were calculated in years A.D., taking into account the time of column chemistry. The isotopic data for all 62 coral samples revealed a range in uranium concentrations from 2.3 to 3.3 ppm (Table 4). Initial δ^{234}U values are within the range of 147 ± 5 per mil (‰), typical of modern seawater and modern or pristine corals reported in other studies (Stirling et al., 1995; Shen et al., 2008; Andersen et al., 2010). Despite rigorous cleaning, concentrations of ^{232}Th in the samples ranged between 0.23 and 18 ppb [mean of 2.7 ± 2.8 (1 sd) ppb], suggesting that there is still a significant amount of detrital Th present in the coral skeleton that has not been fully removed during cleaning. Measured ^{230}Th/^{232}Th values ranged from 0.08 ± 0.01 to 11.39 ± 0.13, and following the correction of initial ^{230}Th using a two-component correction scheme, sample ages become substantially younger compared to their uncorrected ^{230}Th age (by 7.2–131.3 years). Nevertheless, the ^{230}Th ages of replicate samples from colonies PelS2C02-09, HavS1C02.1-09, HavS1C05.1-09, HavS1C17.2-08, HavS3C05.1-09, PanS2C02-09, PanS3C02-09, PanS3C11-08, PanS3C12-08 and PanS3C15-08 all fall within error of each other, indicating remarkable reproducibility between samples. Combining the corrected ^{230}Th age with the number of growth bands above the sampling location for each dead *Porites* colony collected from Pandora Reef, Pelorus and Havannah Island, gave mortality ages at the surface of the colonies ranging from 1753.9 ± 8.1 to 2008.4 ± 2.2 (2σ; Fig. 4). Seventy-percent of the *Porites* colonies gave ^{230}Th ages younger than 1980 A.D., creating two major peaks in the KDE distribution where values fell above the upper limit of the data.

3.2. Elemental ratios

Sr/Ca results in all three sampled colonies display a clear cyclical pattern (Fig. 7) that has been shown to reflect annual SST (e.g. McCulloch et al., 1994). The variation in Sr/Ca in all three colonies ranges from 8.64 to 9.29 mmol mol^{-1} which is similar to values reported in *Porites* corals elsewhere in the GBR (McCulloch et al., 1994; Marshall and McCulloch, 2002; Fallon et al., 2003). The time series represented by the Sr/Ca data spans approximately four full cycles (trough to trough) for the HavS3C03-09 colony, five for the HavS3C02-09 colony and three for the HavS3C06-09 colony, with each cycle representing 1 year of growth.

In the HavS3C06-09 colony, Sr/Ca ratios declined gradually to a low of 8.87 mmol mol^{-1} prior to mortality (Fig. 7a). Mean SST (± standard deviation) prior to mortality was 29.2 ± 0.6 °C ($n = 6$). Variation in Sr/Ca in the HavS3C02-09 colony ended with a high value of 9.09 mmol mol^{-1} at the surface of the colony, corresponding to a SST of 25.7 °C (Fig. 7b). The last four samples in the HavS3C03-09 colony reveal Sr/Ca ratios to be declining after producing a narrow trough with a maximum value of 9.16 mmol mol^{-1}. The last two cycles also show a positive shift towards higher Sr/Ca ratios, resulting in an apparent cooling in SST over a period of 5 years. Minimum SSTs recorded by the coral during the Austral winter periods declined from 26.1 °C approximately 5 years prior to mortality, to 23.4 °C around the time of death (Fig. 7c). When compared to *in situ* instrumental temperature records obtained from loggers at 6.4 m depth at Havannah Island from 2007 to present (AIMS, 2014), the reconstructed SSTs from HavS3C06-09 fall within the range of modern monthly average values (Fig. 7a). Maximum reconstructed SSTs for HavS3C02-09 also fell within the range of modern values, however, minimum SSTs were ~3 °C warmer (Fig. 7b). For the HavS3C03-09 colony, reconstructed SSTs were on average 5 °C warmer (Fig. 7c).

Variation in Mg/Ca was synchronous with Sr/Ca in only the HavS3C06-09 and HavS3C02-09 colonies with a mean (± standard deviation) value of 4.02 ± 0.50 mmol mol^{-1} (Fig. 7d, e). Overall, Mg/Ca ranged between 3.16 and 10.31 mmol mol^{-1}, with greater variation observed in samples taken within ~10 mm of the surface of the colonies. For the HavS3C03-09 colony, no clear annual cycles in Mg/Ca were observed. Mg/Ca values remained constant for the length of the sample with a mean value of 4.60 ± 0.96 mmol mol^{-1}, before increasing exponentially towards the surface of the colony, reaching values up to 10.31 mmol mol^{-1} (Fig. 7f).

Measurements of Ba/Ca varied between 1.56×10^{-6} and 4.56×10^{-5} mol mol^{-1}. In the HavS3C06-09 colony, Ba/Ca ratios fluctuated between 1.69×10^{-6} and 1.25×10^{-5} mol mol^{-1} for the length of the sample, showing a gradual increase towards the surface of the colony (Fig. 7g). In the HavS3C02-09 colony, baseline variability in Ba/Ca was interspersed by two major peaks; the first occurring around sample number 56 and corresponding to the beginning of a peak in Sr/Ca and Mg/Ca. the second occurs towards the surface of the colony, with Ba/Ca values increasing rapidly to 1.39×10^{-5} mol mol^{-1} (Fig. 7h). A similar characteristic can be found at the surface of the HavS3C03-09 colony, where Ba/Ca ratios also increase rapidly to 4.56×10^{-5} mol mol^{-1}; however, no other major peaks are observed for the rest of the time series (Fig. 7i).

Table 4
MC-ICP-MS and TIMS ^{230}Th ages of 50 dead *Porites* collected from the leeward side of Pandora Reef, Pelorus and Havannah Island, central inshore GBR.

Sample name[a]	Sample weight (g)	U (ppm)	^{232}Th (ppb)	$(^{230}Th/^{232}Th)_{meas}$	$(^{230}Th/^{238}U)$	$\delta^{234}U$[c]	Uncorr. ^{230}Th Age (a)	Time of chemistry	Corr.^{230}Th age (AD)[d]	No. growth bands above sampling location[e]	Surface age[f]
Pelorus Island											
PelS1C01-09	0.31976	2.7635 ± 0.0025	18.182 ± 0.042	1.40 ± 0.01	0.003031 ± 0.000023	147.1 ± 1.4	288.9 ± 2.2	2013.62	1856 ± 26	Unclear (<1)	1857 ± 26
PelS1C02.1-09	1.12900	2.6428 ± 0.0032	1.3184 ± 0.0066	1.11 ± 0.04	0.000183 ± 0.000007	148.4 ± 1.3	17.4 ± 0.7	2009.85	2005.7 ± 2.7	~2.5	2008.2 ± 2.7[g]
PelS1C03-09	0.41237	2.5879 ± 0.0020	3.2258 ± 0.0072	1.41 ± 0.03	0.000580 ± 0.000011	147.3 ± 1.6	55.3 ± 1.1	2013.62	1987.7 ± 6.0	Unclear (<1)	1988.7 ± 6.0
PelS2C01-09	0.40378	2.5618 ± 0.0023	0.6615 ± 0.0012	2.05 ± 0.07	0.000175 ± 0.000006	147.3 ± 1.6	16.7 ± 0.6	2013.62	2007.4 ± 2.2	Unclear (<1)	2008.4 ± 2.2[g]
PelS2C02-09	0.93417	3.3307 ± 0.0055	4.9333 ± 0.0038	0.92 ± 0.01	0.000451 ± 0.000006	146.7 ± 0.8	43.0 ± 0.6	2010.24	2000.1 ± 6.6	~1	2001.1 ± 6.6[g]
PelS2C02-09[b]	0.27959	2.8479 ± 0.0026	1.1354 ± 0.0017	2.22 ± 0.07	0.000292 ± 0.000009	146.6 ± 1.8	27.8 ± 0.9	2013.62	1998.4 ± 2.7	1	1999.4 ± 2.7
PelS2C03-08	0.26872	2.8221 ± 0.0015	4.8313 ± 0.0074	5.56 ± 0.06	0.003139 ± 0.000030	147.7 ± 1.3	299.2 ± 2.9	2013.62	1752.4 ± 8.1	~1.5	1753.9 ± 8.1
PelS2C06-09	1.46896	2.5218 ± 0.0023	0.5824 ± 0.0004	1.33 ± 0.02	0.000101 ± 0.000003	147.1 ± 0.8	9.6 ± 0.3	2010.24	2007.8 ± 1.5	1	2008.1 ± 1.5[g]
PelS2C07-09	0.35460	2.6005 ± 0.0026	2.0113 ± 0.0050	1.46 ± 0.03	0.000372 ± 0.000007	147.1 ± 1.8	35.4 ± 0.6	2013.62	1998.4 ± 4.1	Unclear (<3)	2001.4 ± 4.1
PelS3C02-09	0.27257	2.6890 ± 0.0021	3.3846 ± 0.0036	1.90 ± 0.04	0.000790 ± 0.000016	148.0 ± 1.2	75.3 ± 1.5	2013.62	1967.7 ± 6.1	Unclear (<1)	1968.7 ± 6.1
PelS3C03.1-09	1.36111	2.8868 ± 0.0051	0.8006 ± 0.0037	1.37 ± 0.05	0.000125 ± 0.000006	143.8 ± 1.8	12.0 ± 0.6	2009.85	2006.4 ± 1.8	~1.5	2007.9 ± 1.8[g]
PelS3C04-08	0.42363	2.6033 ± 0.0033	1.2087 ± 0.0029	6.06 ± 0.10	0.000929 ± 0.000015	143.9 ± 1.7	88.7 ± 1.4	2013.62	1939.3 ± 3.2	Unclear (<4)	1943.2 ± 3.2
PelS3C06-08	0.50673	2.4767 ± 0.0044	0.5519 ± 0.0011	8.97 ± 0.15	0.000659 ± 0.000011	148.0 ± 1.7	62.7 ± 1.0	2013.62	1960.8 ± 2.2	2	1962.8 ± 2.2
PelS3C07-08	0.34937	2.3614 ± 0.0026	1.6430 ± 0.0027	3.33 ± 0.06	0.000763 ± 0.000014	147.0 ± 1.2	72.7 ± 1.3	2013.62	1960.2 ± 4.1	~1.5	1961.7 ± 4.1
Havannah Island											
HavS1C01.1-09	1.07203	2.7143 ± 0.0034	1.0896 ± 0.0045	1.90 ± 0.05	0.000251 ± 0.000008	146.2 ± 1.6	23.9 ± 0.7	2009.85	1997.2 ± 2.4	~1	1998.2 ± 2.4
HavS1C02.1-09	0.61415	2.7356 ± 0.0021	5.837 ± 0.031	1.02 ± 0.02	0.000717 ± 0.000013	146.0 ± 1.3	68.4 ± 1.3	2009.85	1988.2 ± 9.4	~1	1989.2 ± 9.4
HavS1C02.1-09[b]	0.27683	2.3813 ± 0.0016	6.631 ± 0.015	0.96 ± 0.02	0.000883 ± 0.000017	147.1 ± 1.9	84.0 ± 1.6	2013.62	1989 ± 12	~1	1990 ± 12
HavS1C03.1-09	1.21228	3.1975 ± 0.0043	1.1977 ± 0.0046	5.88 ± 0.11	0.000725 ± 0.000013	145.4 ± 1.5	69.2 ± 1.2	2009.85	1950.9 ± 2.4	~11	1961.9 ± 2.4
HavS1C04-09	0.68305	2.9351 ± 0.0023	4.8967 ± 0.0035	1.05 ± 0.01	0.000575 ± 0.000008	144.8 ± 0.8	54.9 ± 0.8	2010.24	1992.4 ± 7.5	1	1993.4 ± 7.5[g]
HavS1C05.1-09	1.18692	2.6142 ± 0.0041	4.313 ± 0.049	1.49 ± 0.04	0.000812 ± 0.000014	148.8 ± 1.1	77.3 ± 1.3	2010.24	1969.8 ± 7.5	~6	1975.8 ± 7.5
HavS1C05.1-09 [b]	0.23062	2.5653 ± 0.0012	1.2901 ± 0.0022	4.00 ± 0.07	0.000662 ± 0.000010	146.5 ± 1.8	63.2 ± 1.0	2013.62	1965.6 ± 3.2	~6	1971.6 ± 3.2
HavS1C06-09	0.28530	2.3985 ± 0.0019	6.197 ± 0.011	0.97 ± 0.02	0.000828 ± 0.000017	146.9 ± 1.2	78.9 ± 1.6	2013.62	1990 ± 11	Unclear (<1)	1990 ± 11[g]
HavS1C07.1-09	0.97326	2.6063 ± 0.0027	2.0794 ± 0.0125	1.78 ± 0.05	0.000468 ± 0.000013	146.9 ± 1.4	44.6 ± 1.3	2009.85	1984.7 ± 4.1	4.5	1989.2 ± 4.1
HavS1C12.1-08	0.50675	2.8551 ± 0.0034	0.9558 ± 0.0017	3.16 ± 0.05	0.000348 ± 0.000006	142.5 ± 2.2	33.3 ± 0.5	2013.62	1991.7 ± 2.3	Unclear (<3)	1994.7 ± 2.3
HavS1C13-08	0.29429	2.2620 ± 0.0024	1.6279 ± 0.0025	1.82 ± 0.06	0.000431 ± 0.000014	145.3 ± 1.5	41.1 ± 1.3	2013.62	1992.6 ± 4.2	3	1995.6 ± 4.2
HavS1C14-08	0.30394	2.4520 ± 0.0019	1.3117 ± 0.0016	2.10 ± 0.08	0.000371 ± 0.000014	145.5 ± 1.2	35.4 ± 1.3	2013.62	1994.3 ± 3.5	Unclear (<2)	1996.3 ± 3.5
HavS1C15-08	0.41585	2.3958 ± 0.0020	0.9599 ± 0.0013	2.90 ± 0.05	0.000383 ± 0.000007	143.0 ± 1.6	36.6 ± 0.7	2013.62	1990.6 ± 2.8	2	1992.6 ± 2.8
HavS1C16-08	0.49558	2.5475 ± 0.0025	0.2304 ± 0.0004	8.58 ± 0.21	0.000256 ± 0.000006	143.9 ± 1.7	24.4 ± 0.6	2013.62	1996.5 ± 1.6	2.5	1999.0 ± 1.6
HavS1C17.2-08	0.85977	3.2811 ± 0.0046	2.7973 ± 0.0146	1.33 ± 0.03	0.000373 ± 0.000010	147.9 ± 1.6	35.5 ± 0.9	2009.54	1994.0 ± 4.1	3	1997.0 ± 4.1
HavS1C17.2-08 [b]	0.28874	2.4399 ± 0.0015	0.3641 ± 0.0007	5.94 ± 0.18	0.000292 ± 0.000009	142.8 ± 1.6	27.9 ± 0.8	2013.62	1994.4 ± 1.9	2	1996.4 ± 1.9
HavS2C01-09	0.30855	2.8037 ± 0.0027	3.2363 ± 0.0048	5.62 ± 0.05	0.002138 ± 0.000019	145.8 ± 1.8	203.9 ± 1.9	2013.62	1836.9 ± 5.7	Unclear (<1)	1836.9 ± 5.7
HavS2C02-09	1.28689	2.4871 ± 0.0018	0.7126 ± 0.0007	1.54 ± 0.03	0.000145 ± 0.000004	145.1 ± 1.0	13.8 ± 0.4	2010.24	2005.4 ± 1.8	~1	2006.4 ± 1.8[g]
HavS2C02.1-08	0.29966	2.4214 ± 0.0013	1.0031 ± 0.0018	6.93 ± 0.10	0.000947 ± 0.000013	145.5 ± 1.8	90.3 ± 1.2	2013.62	1937.1 ± 3.0	~7.5	1944.6 ± 3.0
HavS3C01-09	0.20233	2.6979 ± 0.0015	2.3809 ± 0.0053	1.70 ± 0.03	0.000496 ± 0.000009	144.7 ± 1.5	47.3 ± 0.9	2013.62	1988.5 ± 4.5	0	1988.5 ± 4.5
HavS3C02.1-09[a]	1.07575	2.9324 ± 0.0032	1.709 ± 0.010	1.13 ± 0.03	0.000217 ± 0.000006	144.2 ± 1.8	20.7 ± 0.6	2009.85	2003.9 ± 3.0	3	2006.9 ± 3.0[g]
HavS3C03.1-09[a]	0.77059	2.8512 ± 0.0021	0.8946 ± 0.0034	1.41 ± 0.06	0.000145 ± 0.000007	144.7 ± 1.0	13.9 ± 0.6	2009.85	2005.3 ± 2.0	3	2008.3 ± 2.0[g]
HavS3C04.1-09	1.10991	2.9486 ± 0.0032	1.1865 ± 0.0059	2.49 ± 0.05	0.000330 ± 0.000007	146.9 ± 1.5	31.5 ± 0.7	2009.85	1989.3 ± 2.3	~6	1995.3 ± 2.3

HavS3C05.1-09	0.98022	2.9911 ± 0.0030	5.693 ± 0.041	1.75 ± 0.05	0.001097 ± 0.000028	146.3 ± 1.4	104.5 ± 2.7	2009.85	1947.1 ± 8.8	1	1948.1 ± 8.8
HavS3C05.1-09 [b]	0.18023	2.3584 ± 0.0018	3.3714 ± 0.0036	2.26 ± 0.04	0.001064 ± 0.000018	147.7 ± 1.1	101.2 ± 1.7	2013.62	1945.8 ± 6.9	1	1946.8 ± 6.9
HavS3C06-09[a]	1.78586	2.8995 ± 0.0039	1.1688 ± 0.0031	2.24 ± 0.04	0.000297 ± 0.000006	145.1 ± 1.7	28.4 ± 0.6	2009.85	1992.6 ± 2.3	2	1994.6 ± 2.3[g]
Pandora Reef											
PanS2C01-09	0.25195	2.6468 ± 0.0020	4.1992 ± 0.0077	1.09 ± 0.02	0.000568 ± 0.000008	145.9 ± 0.7	54.2 ± 0.8	2013.62	1995.2 ± 7.2	Unclear (<1)	1996.2 ± 7.2[g]
PanS2C02-09	1.13562	2.4673 ± 0.0034	5.3606 ± 0.0043	0.93 ± 0.01	0.000666 ± 0.000009	146.9 ± 1.4	63.5 ± 0.8	2010.24	1994.6 ± 9.6	~3	1997.8 ± 9.6[g]
PanS2C02-09 [b]	0.17076	2.2918 ± 0.0011	2.9228 ± 0.0040	1.42 ± 0.04	0.000598 ± 0.000015	148.3 ± 2.2	56.9 ± 1.4	2013.62	1987.2 ± 6.3	~4	1991.2 ± 6.3
PanS3C01.1-08	0.18959	2.6637 ± 0.0013	1.0709 ± 0.0009	2.66 ± 0.08	0.000352 ± 0.000010	146.3 ± 1.7	33.6 ± 1.0	2013.62	1993.1 ± 2.8	1.5	1994.6 ± 2.8
PanS3C01-09	0.51329	2.5308 ± 0.0017	0.2990 ± 0.0004	6.23 ± 0.12	0.000242 ± 0.000005	144.8 ± 1.3	23.1 ± 0.4	2013.62	1998.3 ± 1.6	1	1999.3 ± 1.6
PanS3C02-09	0.77092	2.7713 ± 0.0036	2.8948 ± 0.0034	1.12 ± 0.02	0.000385 ± 0.000007	147.6 ± 1.0	36.7 ± 0.7	2010.24	1997.9 ± 4.9	2	1999.9 ± 4.9[g]
PanS3C02-09 [b]	0.42335	2.4207 ± 0.0012	1.9627 ± 0.0018	1.55 ± 0.02	0.000415 ± 0.000005	147.0 ± 2.3	39.5 ± 0.5	2013.62	1995.5 ± 4.3	2	1997.5 ± 4.3
PanS3C03-09	0.39239	2.5746 ± 0.0021	0.2507 ± 0.0004	11.28 ± 0.32	0.000362 ± 0.000010	146.2 ± 1.7	34.5 ± 1.0	2013.62	1986.4 ± 1.8	Unclear (<8)	1994.4 ± 1.8
PanS3C04-09	1.05471	2.6994 ± 0.0029	8.1708 ± 0.0070	0.80 ± 0.01	0.000802 ± 0.000011	147.6 ± 0.9	76.4 ± 1.0	2010.24	1999 ± 13	~0.5	1999 ± 13[g]
PanS3C05-09	0.50384	2.6624 ± 0.0017	2.4668 ± 0.0036	1.73 ± 0.01	0.000529 ± 0.000004	143.8 ± 1.1	50.5 ± 0.4	2013.62	1986.2 ± 4.6	Unclear (<1)	1987.2 ± 4.6
PanS3C06-09	0.56622	2.7981 ± 0.0048	1.6399 ± 0.0027	5.44 ± 0.10	0.001051 ± 0.000019	145.4 ± 1.7	100.2 ± 1.8	2013.62	1929.7 ± 3.7	Unclear (<4)	1933.7 ± 3.7
PanS3C08.2-09	0.3003	3.3457 ± 0.0026	1.0458 ± 0.0018	3.43 ± 0.09	0.000353 ± 0.000009	145.1 ± 1.6	33.7 ± 0.8	2013.62	1990.1 ± 2.2	1	1991.1 ± 2.2
PanS3C11.1-08	1.01140	2.8472 ± 0.0023	2.6201 ± 0.0080	2.19 ± 0.09	0.000665 ± 0.000026	146.4 ± 1.2	63.4 ± 2.5	2009.54	1967.8 ± 5.0	2.5	1980.3 ± 5.0
PanS3C11.2-08 [b]	1.03371	2.7662 ± 0.0021	1.5893 ± 0.0091	3.90 ± 0.08	0.000739 ± 0.000013	146.3 ± 1.2	70.5 ± 1.3	2009.54	1953.8 ± 3.2	2	1955.8 ± 3.2
PanS3C11.2-08 [b]	0.55837	2.7282 ± 0.0046	0.4932 ± 0.0007	11.39 ± 0.13	0.000679 ± 0.000008	145.8 ± 1.4	64.7 ± 0.8	2013.62	1957.5 ± 1.9	2	1959.5 ± 1.9
PanS3C12.1-08	0.94030	2.5821 ± 0.0019	0.9499 ± 0.0061	1.94 ± 0.07	0.000235 ± 0.000009	146.0 ± 1.2	22.4 ± 0.8	2009.54	1997.8 ± 2.3	~2.5	2000.3 ± 2.3
PanS3C12.2-08 [b]	0.78431	2.5769 ± 0.0022	0.8908 ± 0.0064	2.23 ± 0.07	0.000254 ± 0.000008	145.1 ± 1.4	24.2 ± 0.7	2009.54	1995.5 ± 2.2	2	1997.5 ± 2.2
PanS3C13-08	1.26483	2.8105 ± 0.0021	0.8020 ± 0.0034	2.59 ± 0.07	0.000244 ± 0.000007	145.8 ± 1.2	23.2 ± 0.7	2009.54	1995.0 ± 1.9	3.5	1998.5 ± 1.9
PanS3C14-08	0.71700	2.6157 ± 0.0019	8.547 ± 0.028	1.80 ± 0.05	0.001942 ± 0.000054	145.8 ± 1.2	185.3 ± 5.2	2009.13	1894 ± 15	Unclear (<2)	1896 ± 15
PanS3C14-08 [b]	0.20666	2.4506 ± 0.0015	5.2144 ± 0.0065	2.56 ± 0.04	0.001793 ± 0.000030	150.0 ± 0.6	170.4 ± 2.9	2013.62	1889.6 ± 9.7	Unclear (<2)	1891.6 ± 9.7
PanS3C15-08	1.06282	2.5964 ± 0.0024	3.277 ± 0.016	1.74 ± 0.04	0.000726 ± 0.000017	144.1 ± 1.4	69.3 ± 1.7	2009.13	1968.9 ± 6.0	~3	1971.9 ± 6.0
PanS3C15-08 [b]	0.32103	2.6690 ± 0.0021	1.7681 ± 0.0013	2.92 ± 0.15	0.000638 ± 0.000033	147.4 ± 1.4	60.8 ± 3.1	2013.62	1970.8 ± 4.7	~3	1973.8 ± 4.7

Ratios in parentheses are activity ratios calculated from atomic ratios using decay constants of Cheng et al. (2000). All values have been calculated after mean laboratory blank extraction. All errors reported in this table are quoted as 2σ. Samples with the time of chemistry in 2009 were analysed using TIMS, and those with the time of chemistry in 2010 and 2013 measured by MC-ICP-MS.

[a] Sr/Ca, Mg/Ca and Ba/Ca ratios available.

[b] Duplicate samples from the same *Porites* colony.

[c] $\delta^{234}U = [(^{234}U/^{238}U) - 1] \times 1000$.

[d] ^{230}Th ages corrected using a model two-component correction value based on the equation: $\left(\frac{^{230}Th}{^{232}Th}\right)_{mix} = \left(\left(\frac{^{232}Th_{live}}{^{232}Th_{dead}}\right) \times \left(\frac{^{230}Th}{^{232}Th}\right)_{live}\right) + \left(\left(\frac{^{232}Th_{dead} - ^{232}Th_{live}}{^{232}Th_{dead}}\right) \times \left(\frac{^{230}Th}{^{232}Th}\right)_{sed}\right)$ where $^{232}Th_{dead}$ is the measured ^{232}Th value (ppb) in the non-living coral sample. $^{232}Th_{live}$ is the mean measured ^{232}Th value (ppb) and $^{230}Th/^{232}Th_{live}$ represents or approximates the isotopic composition of the hydrogenous component in the dead coral skeleton with an atomic value of $5.85 \times 10^{-6} \pm 20\%$ (which corresponds to an activity value of $1.08 \pm 20\%$). $^{230}Th/^{232}Th_{sed}$ is the detrital component represented by a mean atomic value of $3.30 \times 10^{-6} \pm 20\%$ (which corresponds to an activity value of $0.61 \pm 20\%$) from isochron derived initial $^{230}Th/^{232}Th$ values obtained from dead *Porites* coral skeletons.

[e] Number of growth bands above sampling location deduced from coral X-rays and Sr/Ca analysis.

[f] Surface age = Corrected ^{230}Th growth band age + number of growth bands above sampling location.

[g] U–Th age of samples with no clear corallite structure provides the maximum age at the time of mortality.

3.3. Sample preservation and scanning electron microscope analysis

All dead *Porites* colonies samples were dated regardless of their preservation status. Many of the samples showed evidence of bioerosion by boring organisms and/or were discoloured by sediments and organics that became trapped in the skeletal matrix either during growth or post-mortem. The area of each coral sample found to be altered or discoloured using Image J analysis, ranged between 9% and 38%. No significant relationship between the ^{230}Th ages and the degree of alteration or preservation state of the corals was found ($r = -0.05$, $P = 0.75$) (see Fig. 3).

The lack of annual cycles in Mg/Ca, increasing Sr/Ca ratios and anomalously high reconstructed SSTs in the colony HavS3C03 was evidence to suggest that early diagenesis was present in the coral skeleton and warranted further investigation. Scanning electron microscope images revealed concentrated cement-filled borings, occupying as much as 80–90% of the coral skeleton towards the surface of the colony (Fig. 8). Individual borings were irregularly shaped and showed no clear orientation.

4. DISCUSSION

4.1. Timing of mortality

U-series ages for 50 massive *Porites* colonies revealed surface ages ranging from 1754 ± 8 to 2008 ± 2 (Table 4; Fig. 4). However, 30.6% of the colonies sampled still retained high amounts of ^{232}Th (>2 ppb), which introduced substantially large errors to the ^{230}Th ages (up to ±26 years) following the correction of initial ^{230}Th in the coral skeleton (Fig. 4a). The ^{230}Th age distribution produced from the Kernel Density Estimates (KDEs) using

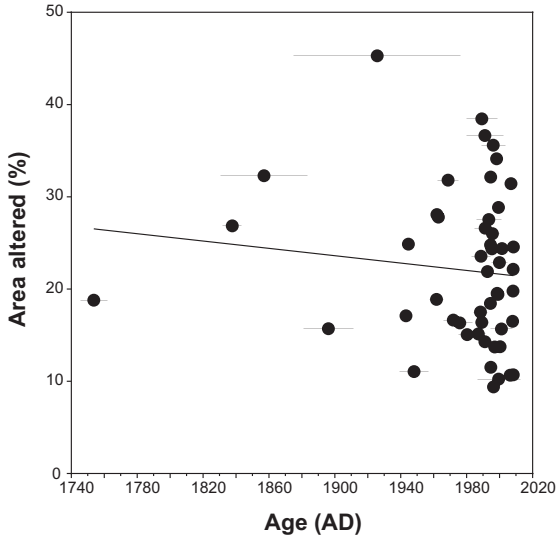

Fig. 3. The area altered (%) versus surface age (years A.D. ±2σ) for each sample taken from 50 *Porites* colonies. Pearson correlation revealed no relationship between the degree of alteration and the age of the coral sample ($r = -0.05$, $P = 0.75$).

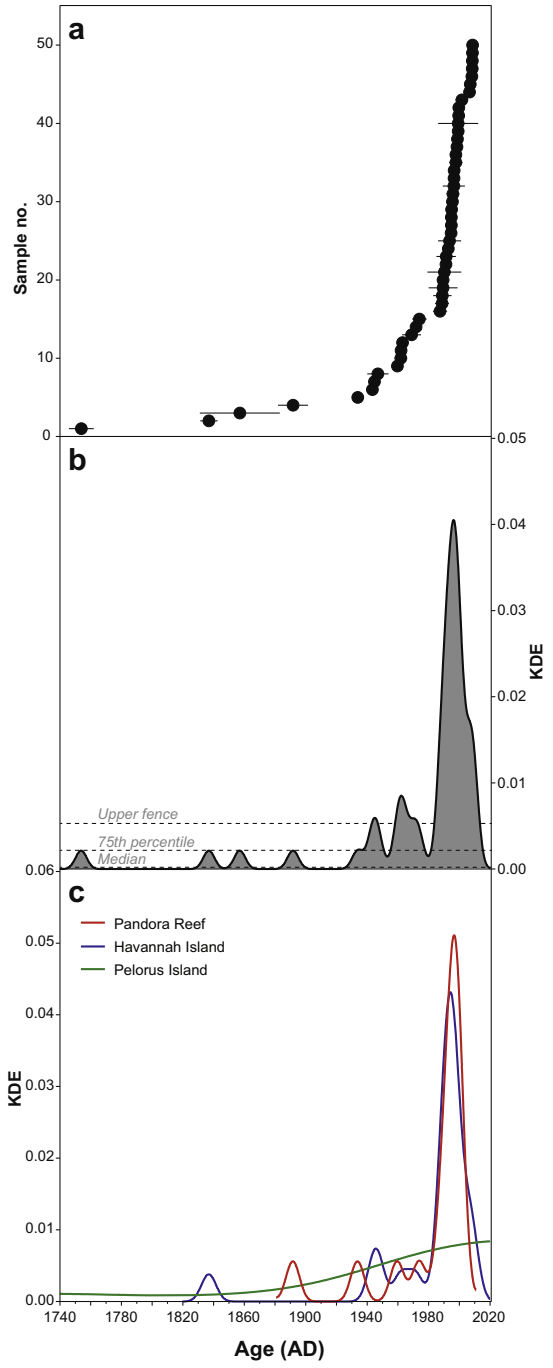

Fig. 4. (a) U–Th ages obtained from colony surfaces through a combination of U–Th dating and 'band-counting' for all 50 individual dead *Porites* skeletons (±2σ error) sampled from the Palm Islands region; (b) KDE distribution produced from all ^{230}Th ages; (c) KDE distributions produced from ^{230}Th ages obtained from *Porites* colonies collected at Pelorus Island (green line), Havannah Island (blue line) and Pandora Reef (red line).The height and width of each Kernel Density Estimate (KDE) reflects a function that stacks a Gaussian 'bell curve' on top of each measurement and whose standard deviation is determined by the local probability density (Vermeesch, 2012). (For interpretation of the references to colour in this figure legend, the reader is referred to the web version of this article.)

all data (excluding one of each of the replicate pairs with ^{232}Th >2 ppb) suggests that major mortality events occurred around ~1942, 1966 and 1997 A.D. Four other peaks are also observed around 1754, 1837, 1857 and 1892 A.D; however, the upper limit of the data (defined as $>Q_3 + 1.5IQR$) that was used for identifying outliers (or in this case, mortality 'events'), suggests that these peaks may not be mortality 'events' *per se*, but rather reflect background mortality, i.e. mortality caused by competition, abrasion and grazing fishes. Also, the peaks between 1740 and 1900 A.D. are represented by only one ^{230}Th age each (Fig. 4). Excluding those samples with high ^{232}Th, the surface ages are constrained to the time period between 1930 and 2009 A.D., and centre around six periods of mortality at ~1934, 1944, 1961, 1973, 1996 and 2008 A.D (Fig. 5d). While the data with ^{232}Th <2 ppb are more reliable (Scholz and Mangini, 2007), only the peak in mortality around ~1996 A.D. is determined to be an outlier and arguably a mortality 'event'. However, it would be erroneous to dismiss the second major peak in the KDE distribution (~2008 A.D.) that falls just short of the upper limit of the KDE values.

In three of the well-preserved colonies with minimal internal and external bioerosion (HavS3C02-09, HavS3C03-09 and HavS3C06-09) from the periods of mortality centred ~1996 and 2008 A.D., elemental ratio analysis was used to further constrain the timing of mortality. Typically, Sr/Ca minima and maxima correspond to SST maxima and minima, respectively (Devilliers et al., 1994; Mitsuguchi et al., 2003). Moreover, the growth characteristics of the coral can also be used to examine seasonal changes in SST with broad, low density bands produced during the austral summer and narrow high-density bands in winter, which can be seen using X-ray images (Knutson et al., 1972; Lough and Barnes, 1990). Examination of X-rays of both the HavS3C02-09 and HavS3C03-09 colonies reveal that a narrow high density band had already been completed, suggesting that mortality occurred after the austral winter/spring and the deposition of a low density band (Fig. 6b, h). This is supported by Sr/Ca variations in the HavS3C03-09 colony, whereby ratios begin to decrease from a maximum Sr/Ca ratio of 9.2 mmol mol^{-1} (Fig. 7c). For the HavS3C02-09 colony, Sr/Ca ratios were approaching values expected for a narrow high-density band (Fig. 7b), suggesting that this colony died prior to the austral winter, contradicting the conclusion drawn from the X-rays. One possible explanation for this is that we were unable to sample the outermost portion of the tissue layer (Yu et al., 2010). Given that both these colonies died around the same time (2006.9 ± 3.0 and 2008.3 ± 2.0 for HavS3C02-09 and HavS3C03-09, respectively) and display similar trace element variations, it is reasonable to argue that both could have died from the same environmental stressor. For the HS3C06-09 colony, the low Sr/Ca ratios suggests that mortality occurred during the austral summer (Fig. 7a) and display a similar pattern to a *Porites* colony sampled from Pandora Reef following the 1998 bleaching event (Marshall and McCulloch, 2002). This is confirmed in the coral X-ray, where a low-density band can be found at the surface of the colony (Fig. 6e).

By combining the ^{230}Th age data and elemental ratio results and comparing with instrumental and proxy data of environmental variables, as well as anecdotal and published reports of disturbances, we assess whether this multi-proxy approach can help to constrain the timing and likely cause of the two major mortality 'events' determined from the dead massive *Porites* colonies.

4.2. Cause for mortality in massive *Porites* corals

There are numerous causes for mortality in massive *Porites* which could have been equally responsible for coral death. Outbreaks of COTS can be responsible for mass mortality of corals (Done, 1987, 1988), yet very few COTS have been recorded using manta tow surveys in the Palm Islands region since surveys began in 1987. Only juvenile COTS have been found at Pelorus Island in 1999 (Thompson and Malcolm, 1999) and Havannah Island during intensive SCUBA surveys following Cyclone Tessi in 2000 (Sweatman et al., 2008). Other possible factors contributing to partial and whole colony mortality in massive *Porites* include outbreaks of disease (Bythell et al., 1993), fish corallivory (Rotjan and Lewis, 2005) and overgrowth by competitive algae (Jompa and McCook, 2003). At Havannah Island, reports of diseased colonies are rare, with incidences of white syndrome only being documented in 2003 (Sweatman et al., 2008). Both black band disease and white syndrome were reported at Pandora Reef for several years prior to 2009, but only at very low levels (Sweatman et al., 2008). While the abundances of many other fish taxa has markedly declined following the dramatic loss of live coral cover following the 1998 bleaching event, the number of grazing and scraping parrotfishes has remained relatively stable at Havannah Island (Sweatman et al., 2008; Cheal et al., 2010). However, chronic low-level corallivory by parrotfish (Bonaldo et al., 2012) is an unlikely explanation for acute mortality as observed in our results. The red filamentous algae (*Anotrichium tenue*) has also been reported to kill coral tissue by active overgrowth on massive *Porites*, with colonies up to 50 cm diameter observed to have been completely killed (Jompa and McCook, 2003). However, the occurrence of affected individuals was not widespread in the Palm Islands (Jompa and McCook, 2003).

While such agents are capable of causing serious injury to the coral colony, mortality is generally localised (see Bythell et al., 1993). The scale of a thermal anomaly or flood event, on the other hand, is much larger and likely to affect a greater number of individuals (see Baird and Marshall, 1998). Therefore, as the ^{230}Th ages obtained in this study from multiple samples and from different sites cluster around the same time period (Fig. 4), this provides further supportive evidence that a widespread environmental perturbation was the likely cause for mortality.

Overall, comparison of the KDE data (<2 ppb ^{232}Th) with various local long-term environmental records revealed a significant relationship only with annual maximum SST anomalies and average annual SST (Table 5), suggesting that the primary driver for mortality in the *Porites* colonies in the Palm Islands region is likely to be caused

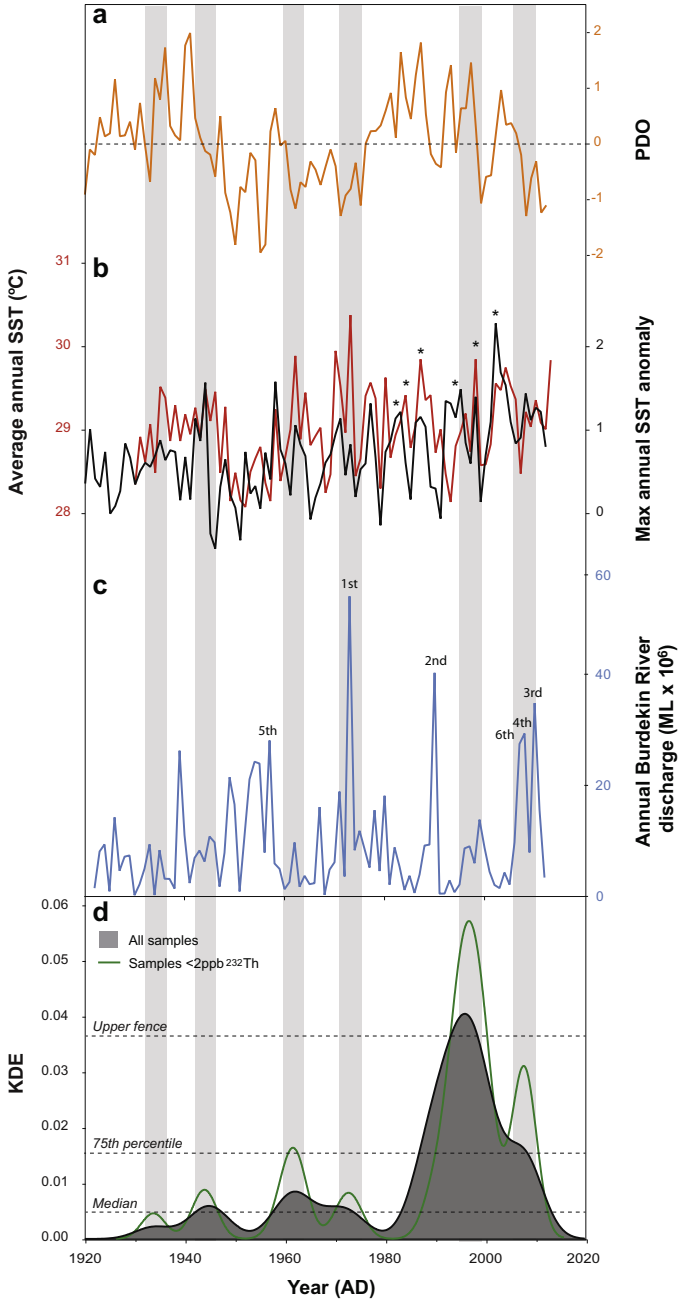

Fig. 5. Summary of environmental factors impacting the Palm Islands region for which there is long-term data and ^{230}Th ages obtained from dead *Porites* colonies from 1920 to 2009. (a) Pacific Decadal Oscillation (source: http://jisao.washington.edu/pdo/PDO.latest). (b) Yearly average sea surface temperatures (HaddSST1) and maximum annual sea surface temperature anomalies (HaddSST2) for 5 × 5 grid 147.5°E, 17.5°S (source: Hadley Centre). Asterisk (*) denotes bleaching years known to have impacted the Palm Islands region (see Supplementary Table S1). (c) Annual Burdekin River discharge in megalitres from the year starting October 1922 to September 2013 measured at the Burdekin River station at Clare site 120006B (source: Queensland Department of the Environment and Resource Management). Numbers above the curve denotes the rank of each flood in terms of the total annual volume of freshwater discharged into the GBR lagoon. Only major floods ranked 1–6 are labelled. (d) KDE distribution of all ^{230}Th ages obtained from 50 dead *Porites* skeletons ($\pm 2\sigma$ error, grey curve) and KDE distribution of ^{230}Th ages with <2 ppb ^{232}Th (green curve). Vertical grey bars highlight periods of mortality constrained by the ^{230}Th ages. (For interpretation of the references to colour in this figure legend, the reader is referred to the web version of this article.)

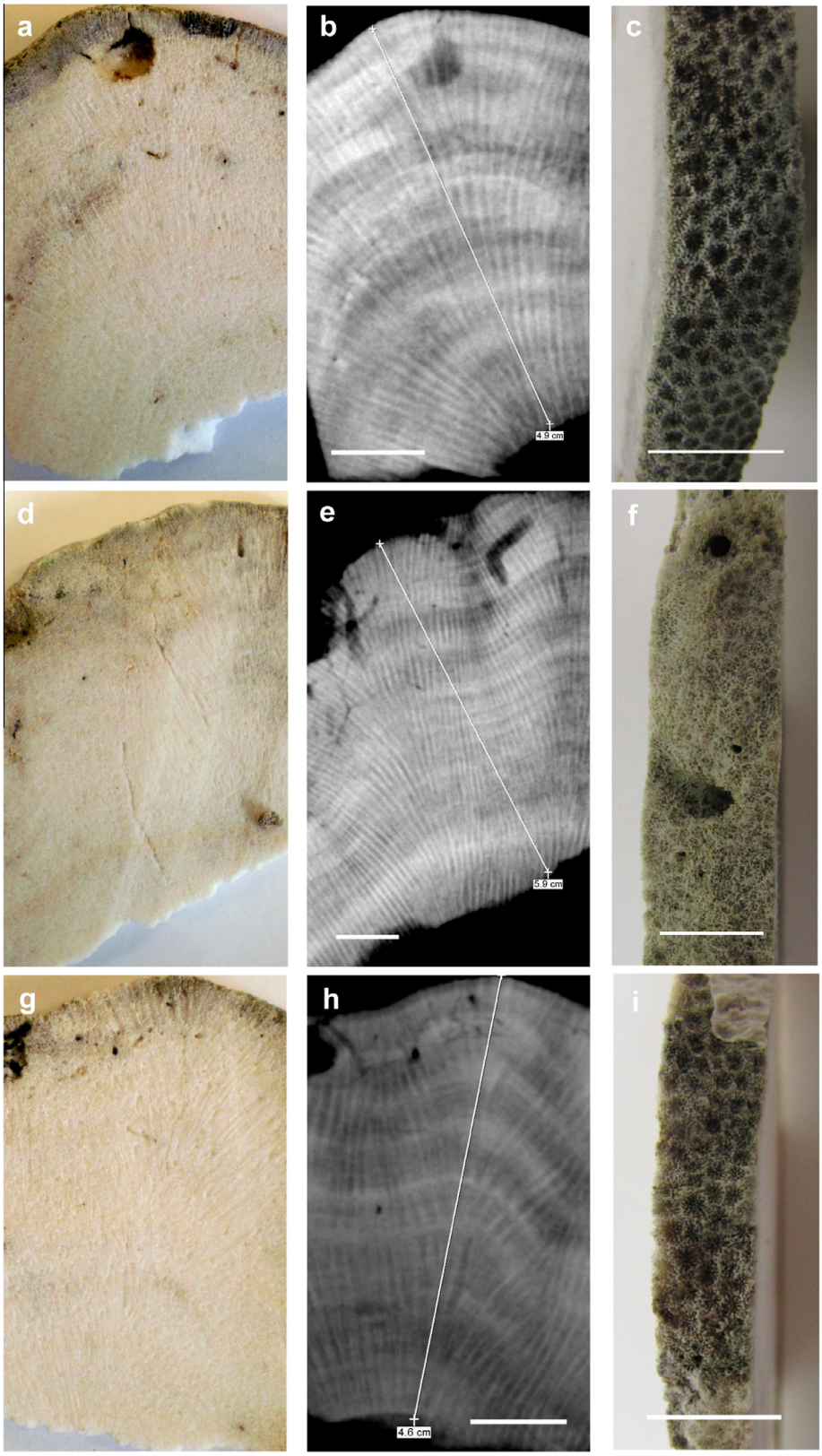

Fig. 6. Photographs and X-ray images of *Porites* samples HavS3C02-09 (a, b, c), HavS3C06-09 (d, e, f) and HavS3C03-09 (g, h, i). Images to the far right reveal clear corallite structure present at the surface of the colonies, suggesting that bioerosion is minimal and that the surface age of the colony (deduced by U–Th dating) is reliable as the time of mortality. Scale bar represents 1 cm.

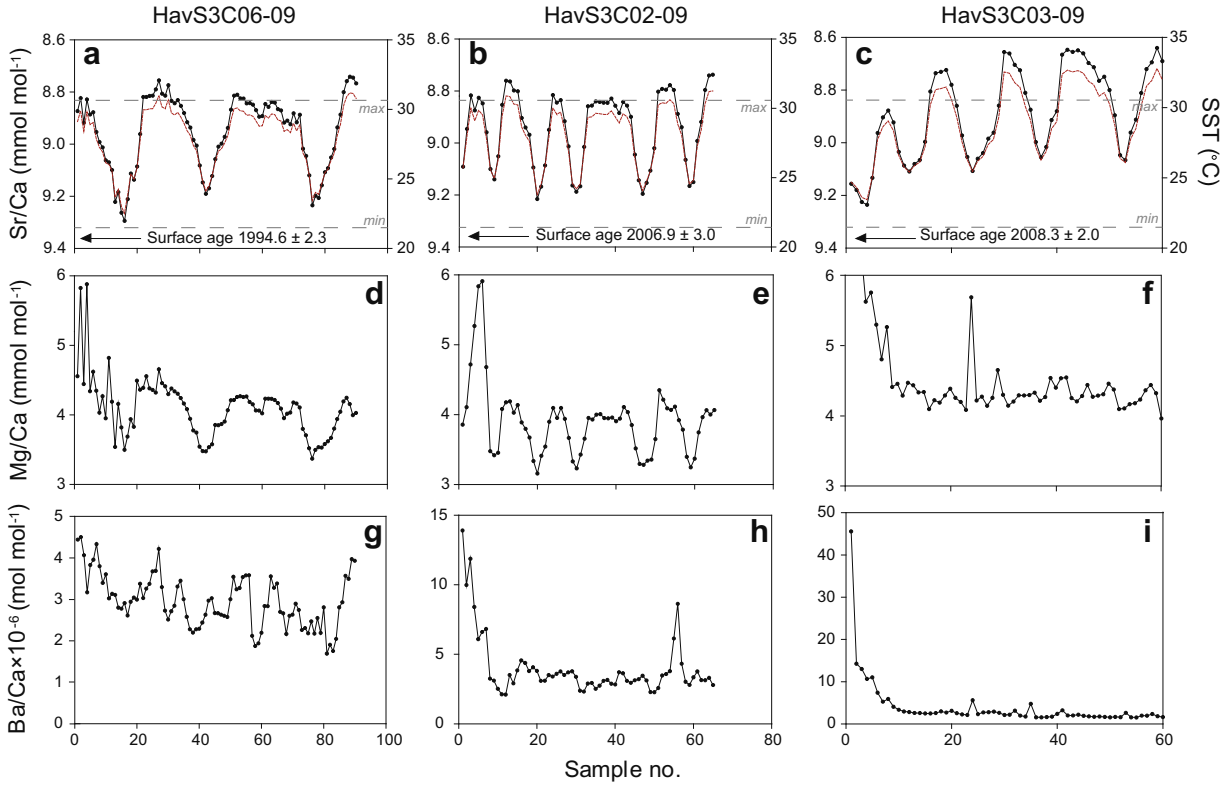

Fig. 7. Sr/Ca and SST, Mg/Ca and Ba/Ca ratios obtained from samples HavS3C06-09 (a, d, g), HavS3C02-09 (b, e, h) and HavS3C03-09 (c, f, i). SSTs (red dotted line) were calculated using the equation $T = 167.9 - [15{,}649\ (Sr/Ca)_{atomic}]$ derived from linear relations between Sr/Ca and temperature for *Porites lutea* colonies from Orpheus Island, GBR (McCulloch et al., 1994; Gagan et al., 1998). The dotted lines reflect the range of modern monthly average SSTs obtained from *in situ* temperature loggers at 6.4 m depth at Havannah Island from 2007 to present (source: AIMS). The plot of Mg/Ca ratios for colony HavS3C03-09 excludes 3 data points (number 1–3) so that the *y*-axis could be enlarged. See Supplementary Tables S2, S3, S4 for data.

by thermal stress. These results are similar to observations made by Yu et al. (2006) where U-series dating of dead *in situ* massive *Porites* corals from Yongshu and Meiji Reefs, southern South China Sea, also revealed simultaneous mortality, suggesting a large scale regional event. Moreover, the ^{230}Th ages coincided with historic El Niño events, implying that mortality may have been caused by high temperature bleaching.

While the overall age distribution produced by the ^{230}Th age data is likely to be due to bleaching induced mortality, we closely examine the two recent major 'events' to ascertain the likely cause for mortality.

4.2.1. First period of mortality (~1996 A.D.)

The first period of major mortality bracketed by 36 colonies in the KDE plot containing all ^{230}Th age data occurred between 1990 ± 11 to 1999 ± 13 (Fig. 4a). This broad range reflects the large age uncertainty associated with samples HavS1C06-09 ($\pm$ 11) and PanS3C04-09 ($\pm$ 13) where ^{232}Th values exceed 2 ppb. This subsequently makes discerning the timing of mortality difficult. If only the samples with ^{232}Th <2 ppb are pooled together (27 of the 36 colonies), the corresponding age range is reduced to between 1989.2 ± 4.1 to 2001.4 ± 4.1, with ^{230}Th ages centred around ~1996. A second more recent peak in mortality also becomes more prominent (Fig. 5d).

Despite numerous cyclones occurring during the time bracketed by the ^{230}Th ages, the *Porites* colonies sampled in this study were all *in situ*, thus mortality associated with dislodgement and transportation can be ruled out. However, flooding associated with cyclones and thermal bleaching can result in widespread mortality (Thompson et al., 2010). In 1994, 1997 and 1998 the Palm Islands received flood waters from the Wet Tropics Rivers and Burdekin River (Devlin et al., 2001), yet only the disturbances occurring in 1994 and 1998 had reportedly influenced local coral communities and caused mortality in massive *Porites* colonies at the depths sampled in this study (Supplementary Table S1).

In late January 1994, bleaching occurred at Pandora Reef and Orpheus Island following intense rainfall associated with Cyclone Sadie, which caused major flooding of nearby coastal rivers, and a period of high sea surface temperatures that lasted for approximately 2 months (DeVantier et al., 1997). Bleaching was most severe at depths <5 m, with approximately 75% of overall coral cover appearing either partially or totally bleached. However, communities up to 10 m depth were also affected and included large massive colonies believed to be more than a century old. While recovery was rapid in most genera with colonies gaining normal pigmentation within a month, evidence of injury was still present in several massive *Porites* colonies (DeVantier et al., 1997).

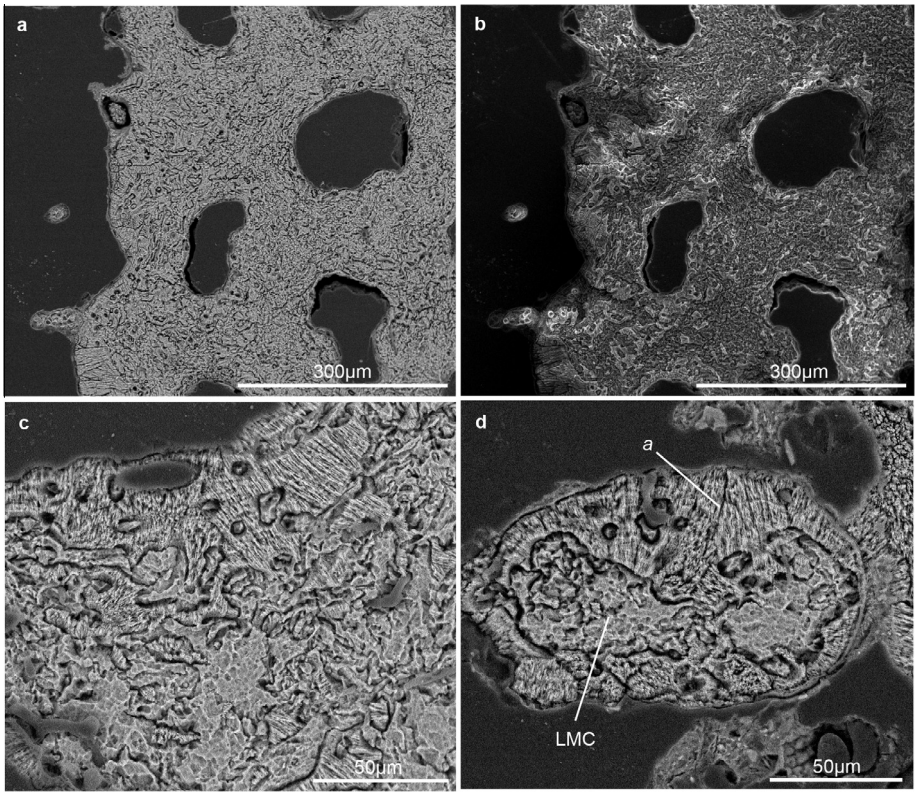

Fig. 8. Scanning electron microscope (SEM) images of a polished and etched section of the coral sample HavS3C03 embedded in resin. (a) Secondary electron image at 400× magnification. (b) Backscattered electron image clearly shows the difference between the borings (dark) and the aragonite needle fibres (light) of the unaltered coral skeleton. Close up of the coral skeleton containing low Mg-calcite (LMC) cements amongst aragonite needles (*a*) at (c) 1500× and (d) 1600× magnification.

Table 5
Pearson correlation coefficients (*r*) of Kernel Density Estimate (KDE) values produced from the ^{230}Th age data versus available long-term environmental records from the Palm Islands region.[a]

Variable	*r* value	*P* value[b]	Correlation period[c]	Source of environmental data
Average annual Ba/Ca (mmol mol^{-1})	−0.1559	0.1878	1925.83–1998.75	McCulloch et al. (2003)
Annual Lucinda precipitation (mm)	−0.0953	0.3886	1925.83–2009.75	BoM[d]
Annual Burdekin River discharge (ML)	−0.0508	0.6460	1925.83–2009.75	BoM[d]
Annual maximum SST anomaly	0.3517	**0.0010**	1926–2010	HaddSST2[e]
Average annual SST (°C)	0.4239	**<0.0001**	1930–2010	HaddSST1[e]

[a] KDE values produced from ^{230}Th ages containing less than 2 ppb ^{232}Th were used.
[b] Bold values indicate significance at $p < 0.05$ level.
[c] KDE values were summed for each year from Oct–Sept for comparison with rainfall and runoff records. KDE values were summed from Jan–Dec for each year for comparison with SST records.
[d] Data obtained from Burdekin River station at Clare site 120006B.
[e] Data obtained for 5 × 5 grid at 17.5°S, 147.5°E.

Even more severe was the unprecedented mass mortality of corals associated with elevated sea surface temperatures in 1997–1998, where approximately 87% of inshore reefs of the GBR were bleached to some extent (Berkelmans and Oliver, 1999). The Palm Islands were among the worst affected, with fringing reefs suffering high mortality, particularly in the family Acroporidae (Baird and Marshall, 1998). Although massive *Porites* were the least affected, 32% of the colonies surveyed experienced moderate bleaching (1–50% of the colony bleached) and a further 30% suffered severe bleaching (>50% of the colony bleached) at Pelorus, Orpheus and Magnetic Island (Marshall and Baird, 2000). Moreover, reports exist of some very large individual corals dying during the event elsewhere in the region (Thompson and Malcolm, 1999; Suzuki et al., 2003).

Given that both events occurred during the austral summer, the trace element data obtained from the HavS3C06-09 colony cannot help to differentiate the two events at the sampling resolution used here. Using a near weekly sampling resolution, it may be possible to closely match the Sr/Ca derived SSTs with the instrumental SST record.

Extreme cooling or heating events characteristic of the time period of interest can then be paired up using the two records and an accurate chronology established (e.g. McCulloch et al., 1994; Marshall and McCulloch, 2002; Hendy et al., 2003a). Moreover, an increase in the number of colonies sampled and ^{230}Th age precision would also help to differentiate the two events.

4.2.2. Second period of mortality (~2008 A.D.)

The most recent period of mortality bracketed by seven *Porites* colonies from Pelorus and Havannah Island occurred between 2006.4 ± 1.8 and 2008.4 ± 2.2 A.D., with ^{230}Th ages clustering around ~2008 A.D. As samples were collected in May 2009, mortality must have occurred prior to this date. This age distribution corresponds with the time period during which two major disturbances occurred (Fig. 5). For the colony HavS2C02-09 which was obviously displaced as a result of strong water movement (Fig. 2), the ^{230}Th age places the time of mortality around 2006.4 ± 1.8 and could be attributed to Cyclone Larry which occurred in March 2006 (Supplementary Table S1). In fact, six of the seven samples have surface mortality ages analytically within error of the time of Cyclone Larry. Yet these colonies were intact at the time of sampling and suggest that off-slope transport is an unlikely cause for mortality.

Despite secondary plumes of flood water from the Tully River impacting the Palm Islands in 2007 and 2008 (Devlin and Schaffelke, 2009), long-term monitoring of major benthic groups suggests that no substantial disturbances occurred between 2005 and 2008, with hard coral cover remaining relatively stable during this time (Johnson et al., 2010). However, in 2007/08 and 2008/09, more than 27×10^6 and 29×10^6 ML of water was discharged into the GBR lagoon from the Burdekin River mouth, equating to the 6th and 4th largest discharge event since 1950/1951, respectively (Fig. 5c). The plume waters associated with both flood events extended past the mid-shelf reefs and the Palm Islands group and lasted for more than 2 months (Devlin et al., 2010), which may have been responsible for the decrease in benthic cover at some sites between 2008 and 2009 (Thompson et al., 2010). The effects of terrestrial runoff on corals are well documented, with increased nutrients, sedimentation, turbidity and pollutants having several direct effects on the physiology and overall survival of affected colonies (for review see Fabricius, 2005).

Using Ba/Ca ratios as a proxy for terrestrial influence, McCulloch et al. (2003) found that significant peaks in Ba/Ca measured in *Porites* skeletons from Havannah and Pandora Reefs correspond to major flood events. Baseline Ba/Ca ratios following European settlement (c.1862) fluctuate around $4–5 \times 10^{-6}$ mol mol^{-1} and can increase to 15×10^{-6} mol mol^{-1} during periods where discharge of suspended sediments to the inner GBR is large, such as the major flood of 1988 (McCulloch et al., 2003). In the colonies investigated in this study, Ba/Ca ratios increase from a baseline level of $2–5 \times 10^{-6}$ to over 40×10^{-6} mol mol^{-1} prior to mortality, however, it is not known whether this signal reflects the incorporation of dissolved Ba into the coral carbonate skeleton (Lea et al., 1989) during a flood event or the post-mortem accumulation of Ba-rich particulates (Lea and Boyle 1993). The fact that the older colony HavS3C06-09 does not contain the same signature is supportive evidence for the former as a substantial amount of time had already passed since the time of mortality in 1994.6 ± 2.3 A.D. to allow for Ba-rich particulates to accumulate. In addition, the outermost discoloured layer of each colony was avoided during sampling and all colonies were rigorously cleaned to remove extraneous phases of Ba residing in detrital clays and organic matter (Lea et al., 1989; Lea and Boyle, 1993). High spatial resolution geochemical analyses (e.g. electron micro-probe analysis (EMPA; Mallela et al., 2011) may help to better understand the anomalous Ba signal, while the analysis of various other proxies such as rare earth elements (REE), δ^{15}N and luminescence may provide further information as to whether riverine input was the primary cause for mortality.

Regardless, the gradual increase in Sr/Ca ratios and anomalous reconstructed SSTs in the HavS3C03-09 colony (which died in 2008.3 ± 2.0 A.D.) is further evidence of stressful conditions prior to mortality (Fig. 7c). Both extreme temperature conditions and flood events have been reported to result in an upwards shift in Sr/Ca ratios attributed to the disruption in transport behaviour of Ca and Sr to the coral skeletal lattice (Marshall and McCulloch, 2002; Fallon et al., 2003). Therefore, the most parsimonious explanation is that stressful conditions associated with the 2008–2009 floods was the cause for the anomalous geochemical signatures and subsequent mortality in the *Porites* colonies HavS3C03-09 and HavS3C02-09.

While it is convincing that factors associated with flooding were a major driver for mortality ~2008 A.D., it begs the question as to why there are no large peaks in mortality associated with previous major flood events; especially around 1973/74, 1990/91, and 1957/58 which correspond to the 1st, 2nd and 5th largest Burdekin River flood events since 1922 A.D. (the third largest flood event occurred in 2010–2011 after sampling took place)? Possible reasons for the lack of ^{230}Th ages around these time periods include: (1) *Porites* are generally robust and able to withstand poor water quality conditions; (2) the latest events occurring between October 2007 and September 2009 are unprecedented in the past 91 years of stream monitoring, with two major flood events occurring in close succession. Prior to this, 2001–2007 was reported to be one of the driest periods comparable to the Federation Drought that occurred in the late 1890s to early 1900s (DNRW, 2007). As a result, it is possible that an increase in rainfall led to large amounts of eroded sediments that had built up during the drought, being transported to GBR waters which caused substantial stress to local coral communities; (3) the effects of recent flood events have been exacerbated by a decline in water quality since European settlement (Roff et al., 2013); (4) a decline in water quality coupled with increasing SSTs may have lowered the resilience of *Porites* colonies to withstand acute flood events (Wooldridge and Done, 2009).

4.3. Bias towards recent events?

Porites colonies may be buried as reefs accrete, become dislodged during storm events or broken down by bioeroding

processes. Remnant tissue of injured colonies may also grow back and conceal areas of the colony that died during previous disturbance events, contributing some bias towards sampling only the most recent mortality events. Therefore, over what time period can the methods described here reliably capture the history of past mortality events?

High reef accretion rates have been reported in the Palm Islands (from 7.2 ± 1.2 m/ka^{-1} (Roff, 2010) to >14 m/ka^{-1} [(Hopley and Barnes, 1985; Johnson and Risk, 1987; Roff, 2010)], theoretically giving a time window of between 71 and 167 years to reconstruct disturbance history in medium sized colonies ~100 cm in diameter (assuming a minimum and maximum accretion rate of 0.6–1.4 cm year^{-1}, respectively). Sampling in this study also took place on the leeward (sheltered) side of each reef, thus limiting the possibility of transportation.

Knowledge of bioerosion rates is especially important when interpreting isotopic ages from dead *Porites* corals, however, they are difficult to constrain. After a colony dies, the skeleton is infiltrated by a suite of boring organisms and is subject to grazing fishes which remove the outer layers of the colony. Therefore, the surface age of the coral can only provide the maximum age at the time of mortality when little is known about the extent of bioerosion above the surface. Rates of bioerosion on the GBR have been found to be lower when compared to reefs in other parts of the world, with net rates increasing with distance from the coast (Tribollet and Golubic, 2005), yet values are generally quoted as the amount of $CaCO_3$ eroded over a certain area per unit in time (i.e. kg m^{-2} year^{-1}) with studies only being conducted over a short period of time. As bioerosion is not a linear function, these values cannot be extrapolated past the duration of the study period. Even for erosion rates to be applicable to this study, estimates in mm year^{-1} are necessary, and are further confounded by the fact that bioerosion is not uniform over an entire colony. Nevertheless, the presence of corallites in a colony that died ~18 years ago (HavS3C06-09 1994.2 ± 2.3 A.D.) suggests that bioerosion rates could be low.

Remnant tissue of injured colonies may also grow back over and conceal areas of the colony that died during previous disturbance events, with coring the colony the only way to capture these events. Hendy et al. (2003a,b) determined the likelihood of observing past mortality events equivalent in intensity and scale to the 1998 bleaching event in cores taken from massive *Porites* colonies to be low. Nevertheless, this study would benefit from future work involving intensive coring of *Porites* colonies to expand the sample population. In consideration of the above factors, the methods used here may be limited to the past ~150 years of history. Fortunately, it is this time period that can help us to understand the response of *Porites* to increasing anthropogenic influence since c.1850.

4.4. Diagenesis: hindrance or help?

While most studies use paleothermometers such as Sr/Ca and Mg/Ca to reconstruct sea surface temperatures, the purpose of this study was to provide some understanding as to which season mortality occurred in the massive *Porites* colonies. It is well known that for paleoclimate reconstructions to be valid, one of the key requisites is that the original elemental and stable isotope inventories in the coral skeleton must not be altered by diagenesis (Nothdurft and Webb, 2009b). The anomalous Mg/Ca and Sr/Ca ratios obtained from the HavS3C03-09 colony (2008.3 ± 2.0 A.D.) relative to the other coral records in the present study, is an indicator that diagenetic alteration, such as the precipitation of low-magnesium calcite cement, may have occurred (McGregor and Gagan, 2003; Quinn and Taylor, 2006; Hendy et al., 2007).

Results of scanning electron microscopy revealed the skeleton to contain a large number of low-Mg calcite filled borings similar to that described by Nothdurft et al. (2007) and Nothdurft and Webb (2009b) in corals collected from Heron Reef, southern GBR. At low concentrations, it appears as though the annual cycles in Mg/Ca such as that observed in the other two colonies, are averaged out to a constant ratio between values typical of the host coral skeletal aragonite and the low Mg-calcite cements, suggesting sub-centimeter scale redistribution of Mg without significant effects on the Sr/Ca pattern. Towards the surface of the colony the concentration of low Mg-calcite cements increases, resulting in an increase in Mg/Ca ratios up to 9.43 mmol mol^{-1} (Fig. 7f), which is similar to observations made elsewhere (Nothdurft et al., 2007). Early diagenesis in scleractinian coral skeletons has been documented within recently dead and even live-collected skeletons, with aragonite needle cements being the most common form of alteration. However, few have documented low Mg-calcite cements in extremely young coral samples similar to that documented here (with the exception of Nothdurft et al., 2007; Nothdurft and Webb, 2009b). The environment necessary for the precipitation of low-Mg calcite cement is likely created by the presence of some microbes (Nothdurft et al., 2007) and while the presence of cements is detrimental to the interpretation of paleoclimate studies, it may well prove as a useful indicator of coral stress prior to mortality. For example, cements and borings have been found to be minimal or absent in long sections of core obtained from large *Porites* colonies that grew in deep (>5 m) water environments or areas characterised by strong currents and open ocean waters (Linsley et al., 2000; Meibom et al., 2003). Nothdurft and Webb (2009a,b) proposed that the excellent preservation of these colonies reflect ideal conditions suitable for continuous coral growth, enabling the colony to outgrow microbial infestations. In the colonies investigated in this study, stressful conditions caused by enhanced turbidity and increased sea surface temperatures may have reduced coral growth and allowed for the infiltration of micro-endoliths [such as those seen by McClanahan et al. (2009) following bleaching in massive *Porites* colonies], which in turn create cement-producing microenvironments suitable for the precipitation of high volumes of low Mg-calcite cements (Nothdurft and Webb, 2009b). Alternatively, Fine and Loya (2002) reported an increase in endolithic algae harbouring the skeleton of the encrusting coral *Oculina patagonica* following bleaching. Once the endosymbiotic algae (zooxanthellae) are expelled, higher light intensities are able to penetrate the coral skeleton resulting in the appearance

of dense green bands or zones containing a high biomass of endolithic filamentous algae near the surface of the coral colony (Highsmith, 1981). These endoliths are also found in massive coral species (Highsmith, 1981; Shashar et al., 1997), and any evidence of these 'blooms' in the form of high density Mg-calcite cements within the coral skeleton, could potentially be a useful proxy for coral condition in the fossil record.

It is also interesting to note that HavS3C03-09 is the youngest (2008.3 ± 2.0 A.D.) among all three colonies with elemental ratio analyses; yet it is this colony that has been most severely affected by diagenesis, to a degree that Mg/Ca annual cycles were not observed. This suggests that rates of diagenesis and bioerosion are controlled by the micro-environment at a colony scale.

5. CONCLUSIONS

The ^{230}Th age distribution obtained from 50 dead massive *Porites* corals sampled from the Palm Islands region was found to significantly correlate with maximum SST anomalies and high average annual SSTs, suggesting that high-temperature induced bleaching may have been predominately responsible for mortality. Excluding those samples which contained ^{232}Th >2 ppb, our results indicate two distinct periods of mortality that occurred between 1989.2 ± 4.1 and 2008.4 ± 2.2 A.D. spanning multiple reefs. The first period of mortality occurred between 1989.2 ± 4.1 to 2001.4 ± 4.1 (2σ), with the ^{230}Th age distribution centred around ~1996, coinciding with the 1997–1998 mass bleaching event. The second more recent period of mortality occurred from 2006.4 ± 1.8 to 2008.4 ± 2.2 at both Havannah and Pelorus Island, with the age distribution centred around ~2008. This time period overlaps with the 4th and 6th largest flood events reported for the Burdekin River in the past 91 years (the largest occurring during the austral summer of 1973–1974). An evaluation of Sr/Ca ratios from two large *in situ* colonies, suggests that both died during, or more likely, shortly after the winter minimum. As both floods occurred during the summer maximum, this may either reflect a lag time between colony stress and mortality or the inability to sample the uppermost layer of the colony. While an increase in Ba/Ca ratios prior to mortality further supports factors associated with the 2008–2009 floods as the primary cause of death, further investigation is needed to assess whether an increase in Ba/Ca reflects riverine input or is the result of the post-mortem accumulation of Ba-rich particulates. Other proxies for terrestrial influence such as luminescence and rare earth elements, combined with scanning electron microscopy may help to determine whether dissolved Ba was directly incorporated into the skeleton and represents a true flood signal. Thus, while the elemental ratios used here may further refine the *timing* of coral mortality at a seasonal resolution, they do not provide further evidence to identify the likely *cause* for mortality.

While the approach taken here works well with young samples with adequate preservation, in less well-preserved specimens, accurately determining the age of older colonies that have remained exposed to bioeroding processes may be more difficult without some knowledge of bioerosion rates. It is also important to note that as our study focused on colonies present at the sediment water interface, our sampling strategy may be biased towards sampling more recent mortality events. However, we argue that this method provides a reliable reconstruction of mortality events for at least the past ~150 years. For colonies that exhibit partial mortality or evidence of multiple scar patterns, such as those caused by COTS outbreaks in different years (DeVantier and Done, 2007), multiple ^{230}Th ages sampled from within a single colony may help to provide a better estimate for the time of death.

Although long-term monitoring suggests that poritid-dominated communities (which include massive and finger *Porites*, *Goniopora* and *Alveopora*) have had relatively stable trajectories of coral cover over the past 25 years since monitoring began (Done et al., 2007; Sweatman et al., 2008), it is not clear how individual massive *Porites* colonies have responded to disturbance. The life-history strategies, ecological and archival value signify the importance of closely monitoring mortality in massive *Porites*. Here we have shown that the application of U–Th dating and elemental analysis to understanding historical mortality events is a powerful combination that may prove useful in this regard. Overall, the results of this study suggest that concomitant mortality events in massive *Porites* occurred not only at least twice in recent years, but also at multiple reef sites at the same time in the Palm Islands region. As a result, the preponderance of ages ranging from the mid-1990s to present in this study raises questions as to whether there has been an increase in *Porites* mortality since European settlement (c. 1850 A.D.).

ACKNOWLEDGEMENTS

This study was partially funded by the Marine and Tropical Sciences Research Facility (MTSRF) Project 1.1.4 'Dating and mapping historical changes in Great Barrier Reef coral communities' to J.-x. Zhao, J.M. Pandolfi and T. Done, the NERP Tropical Ecosystems Hub Project 1.3 'Characterising the cumulative impacts of global, regional and local stressors on the present and past biodiversity of the GBR' to J.-x. Zhao, J.M. Pandolfi, G. Roff, Y.-x. Feng, T. Done and T. Clark, a 2009 Great Barrier Reef Marine Park Authority Science for Management Award and an Australian Postgraduate Award to T. Clark. The majority of the U–Th dates were determined on the Nu Plasma MC-ICP-MS, which was funded by an Australian Research Council LIEF grant (LE0989067) to J.-x. Zhao, J. M. Pandolfi, Y.-x. Feng and others. The manuscript was completed while T. Clark was holding a Research Officer position funded by the NERP project. SEM work completed at QUT was funded by Australian Research Council grant DP1096184 to L. Nothdurft. For field assistance, the authors would like to gratefully acknowledge P. Rachello-Dolmen, C. Reymond, B. Beck, E. Mollee, N. Englebert and management staff of Orpheus Island Research Station (OIRS). Special thanks also to A. Ngyuen for help with trace element analysis.

APPENDIX A. SUPPLEMENTARY DATA

Supplementary data associated with this article can be found, in the online version, at http://dx.doi.org/10.1016/j.gca.2014.04.022.

REFERENCES

Abram N. J., Gagan M. K., McCulloch M. T., Chappell J. and Hantoro W. S. (2003) Coral reef death during the 1997 Indian Ocean dipole linked to Indonesian wildfires. *Science* **301**, 952–955.

Abramoff M. D., Magalhaes P. J. and Ram S. J. (2004) Image Processing with ImageJ. *Biophotonics Int.* **11**, 36–42.

Amelin Y., Kaltenbach A., Iizuka T., Stirling C. H., Ireland T. R., Petaev M. and Jacobsen S. B. (2010) U–Pb geochronology of the solar system's oldest solids with variable $^{238}U/^{235}U$. *Earth Planet. Sci. Lett.* **300**, 343–350.

Andersen M. B., Stirling C. H., Zimmermann B. and Halliday A. N. (2010) Precise determination of the open ocean $^{234}U/^{238}U$ composition. *Geochem. Geophys. Geosyst.* **11**. http://dx.doi.org/10.1029/2010GC003318.

Australian Institute of Marine Science (2014) HAVSL1 Water Temperature @5m Reef Slope Site 1WTEMP 23/6/2011. <http://data.aims.gov.au/aimsrtds/data-tool.xhtml?qc=level2&channels=1835> (accessed 31/10/2013).

Baird A. H. and Marshall J. (1998) Mass bleaching of corals on the Great Barrier Reef. *Coral Reefs* **17**, 376.

Beck J. W., Edwards R. L., Ito E., Taylor F. W., Recy J., Rougerie F., Joannot P. and Henin C. (1992) Sea-surface temperature from coral skeletal strontium calcium ratios. *Science* **257**, 644–647.

Bellwood D. R., Hughes T. P., Folke C. and Nystrom M. (2004) Confronting the coral reef crisis. *Nature* **429**, 827–833.

Berkelmans R. and Oliver J. K. (1999) Large-scale bleaching of corals on the Great Barrier Reef. *Coral Reefs* **18**, 55–60.

Bonaldo R. M., Welsh J. Q. and Bellwood D. R. (2012) Spatial and temporal variation in coral predation by parrotfishes on the GBR: evidence from an inshore reef. *Coral Reefs* **31**, 263–272.

Bythell J. C., Gladfelter E. H. and Bythell M. (1993) Chronic and catastrophic natural mortality of 3 common Caribbean reef corals. *Coral Reefs* **12**, 143–152.

Carilli J. E., Norris R. D., Black B., Walsh S. M. and McField M. (2010) Century-scale records of coral growth rates indicate that local stressors reduce coral thermal tolerance threshold. *Global Change Biol.* **16**, 1247–1257.

Cheal A. J., MacNeil M. A., Cripps E., Emslie M. J., Jonker M., Schaffelke B. and Sweatman H. (2010) Coral-macroalgal phase shifts or reef resilience: links with diversity and functional roles of herbivorous fishes on the Great Barrier Reef. *Coral Reefs* **29**, 1005–1015.

Cheng H., Edwards R. L., Hoff J., Gallup C. D., Richards D. A. and Asmerom Y. (2000) The half-lives of uranium-234 and thorium-230. *Chem. Geol.* **169**, 17–33.

Clark T. R., Roff G., Zhao J. -x., Feng Y. -x., Done T. J. and Pandolfi J. M. (submitted for publication) Testing the accuracy of high-precision U–Th dating of a coral graveyard: a tool for reconstructing historical mortality events in coral reefs. *Quat. Geo*.

Clark T. R., Zhao J-x., Feng Y-x., Done T., Jupiter S., Lough J. and Pandolfi J. M. (2012) Spatial variability of initial $^{230}Th/^{232}Th$ in modern *Porites* from the inshore region of the Great Barrier Reef. *Geochim. Cosmochim. Acta* **78**, 99–118.

Cobb K. M., Charles C. D., Cheng H., Kastner M. and Edwards R. L. (2003) U–Th-dating living and young fossil corals from the central tropical Pacific. *Earth Planet. Sci. Lett.* **210**, 91–103.

Cooper M., Shields G., Faithful J. and Zhao J. (2006) Using Sr/Nd isotopic ratios to determine sediment sources in the Burdekin falls dam, Queensland, Australia. *Geochim. Cosmochim. Acta* **70**. A112–A112.

DeVantier L. M., Turak E. I., Done T. J. and Davidson J. (1997) The effects of Cyclone Sadie on coral communities of nearshore reefs in the central Great Barrier Reef. In *Cyclone Sadie flood plumes in the Great Barrier Reef lagoon: Composition and consequences. Great Barrier Reef Marine Park Authority Workshop Series 22* (ed. A. Steven). Great Barrier Reef Marine Park Authority, Townsville, pp. 65–88.

DeVantier L. M. and Done T. J. (2007) Inferring past outbreaks of the crown-of-thorns seastar from scar patterns on coral heads. In *Geological Approaches to Coral Reef Ecology* (ed. R. B. Aronson). Springer, New York, pp. 85–125.

Devilliers S., Shen G. T. and Nelson B. K. (1994) The Sr/Ca-temperature relationship in coralline aragonite – influence of variability in (Sr/Ca) seawater and skeletal growth parameters. *Geochim. Cosmochim. Acta* **58**, 197–208.

Devlin M., Waterhouse J., Taylor J. and Brodie J. (2001) Flood plumes in the Great Barrier Reef: spatial and temporal patterns in composition and distribution. In *Research Publication No. 68*. Great Barrier Reef Marine Park Authority, Townsville.

Devlin M. and Schaffelke B. (2009) Spatial extent of riverine flood plumes and exposure of marine ecosystems in the Tully coastal region, Great Barrier Reef. *Mar. Freshwater Res.* **60**, 1109–1122.

Devlin M., Waterhouse J., McKinna L. and Lewis S. E. (2010) Terrestrial runoff in the Great Barrier Reef: Marine Monitoring Program (3.7.2b) Tully and Burdekin case studies. Australian Centre for Tropical Freshwater Research, Townsville. p. 87.

Department of Natural Resources and Water (DNRW) (2007) The South East Queensland Drought to 2007. Queensland Government Climate Change Centre of Excellence, Brisbane.

Done T. (1987) Simulation of the effects of *Acanthaster planci* on the population structure of massive corals in the genus *Porites*: evidence of population resilience? *Coral Reefs* **6**, 75–90.

Done T. J. (1988) Simulation of recovery of pre-disturbance size structure in populations of *Porites* spp. damaged by the crown of thorns starfish *Acanthaster planci*. *Mar. Biol.* **100**, 51–61.

Done T. (1992) Constancy and change in some Great Barrier Reef coral communities: 1980–1990. *Am. Zool.* **32**, 655–662.

Done T. J. and Potts D. C. (1992) Influences of habitat and natural disturbances on contributions of massive *Porites* corals to reef communities. *Mar. Biol.* **114**, 479–493.

Done T., Turak E., Wakeford M., DeVantier L. M., McDonald A. and Fisk D. (2007) Decadal changes in turbid-water coral communities at Pandora Reef: loss of resilience or too soon to tell? *Coral Reefs* **26**, 789–805.

Edwards R. L., Chen J. H. and Wasserburg G. J. (1987) ^{238}U–^{234}U–^{230}Th–^{232}Th systematics and the precise measurement of time over the past 500,000 years. *Earth Planet. Sci. Lett.* **81**, 175–192.

Endean R. and Cameron A. M. (1985) Ecocatastrophe on the Great Barrier Reef. In *Proceedings of the Fifth International Coral Reef Congress*. Tahiti. pp. 309–314.

Fabricius K. A. (2005) Effects of terrestrial runoff on the ecology of corals and coral reefs: review and synthesis. *Mar. Pollut. Bull.* **50**, 125–146.

Fallon S. J., McCulloch M. T. and Alibert C. (2003) Examining water temperature proxies in *Porites* corals from the Great Barrier Reef: a cross-shelf comparison. *Coral Reefs* **22**, 389–404.

Ferguson C. A. (2008) Nutrient pollution and the molluscan death record: use of mollusc shells to diagnose environmental change. *J. Coastal Res.* **24**, 250–259.

Fine M. and Loya Y. (2002) Endolithic algae: An alternative source of photoassimilates during coral bleaching. *Proc. R. Soc. B-Bio.* **269**, 1205–1210.

Furnas M. (2003) *Catchments and Corals: Terrestrial Runoff to the Great Barrier Reef*. Australian Institute of Marine Science, Townsville.

Gagan M. K., Ayliffe L. K., Hopley D., Cali J. A., Mortimer G. E., Chappell J., McCulloch M. and Head M. J. (1998) Temperature and surface-ocean water balance of the mid-Holocene tropical western Pacific. *Science* **279**, 1014–1018.

Gagan M. K., Ayliffe L. K., Beck J. W., Cole J. E., Druffel E. R. M., Dunbar R. B. and Schrag D. P. (2000) New views of tropical palaeoclimates from corals. *Quatern. Sci. Rev.* **19**, 45–64.

Glynn P. W. (1983) Extensive bleaching and death of reef corals on the Pacific coast of Panama. *Environ. Conserv.* **10**, 149–154.

Hellstrom J. (2003) Rapid and accurate U–Th dating using parallel ion-counting multi-collector ICP-MS. *J. Anal. Atom. Spectrom.* **18**, 1346–1351.

Hendy E. J., Gagan M. K. and Lough J. M. (2003a) Chronological control of coral records using luminescent lines and evidence for non-stationary ENSO teleconnections in northeast Australia. *Holocene* **13**, 187–199.

Hendy E. J., Lough J. M. and Gagan M. K. (2003b) Historical mortality in massive *Porites* from the central Great Barrier Reef, Australia: evidence for past environmental stress? *Coral Reefs* **22**, 207–215.

Hendy E. J., Gagan M. K., Lough J. M., McCulloch M. and deMenocal P. B. (2007) Impact of skeletal dissolution and secondary aragonite on trace element and isotopic climate proxies in Porites corals. *Paleoceanography* **22**, PA4101, doi:10.1029/2007PA001462.

Highsmith R. C. (1981) Lime-boring algae in hermatypic coral skeletons. *J. Exp. Mar. Biol. Ecol.* **55**, 267–281.

Hopley D. and Barnes D. (1985) Structure and development of a windward fringing reef, Orpheus Island, Palm Group, Great Barrier Reef. In: *Proceedings of the 5th International Coral Reef Congress*, vol. **3**. Tahiti. pp. 141–146.

Hughes T. P. and Jackson J. B. C. (1985) Population dynamics and life histories of foliaceous corals. *Ecol. Monogr.* **55**, 141–166.

Hughes T. P., Baird A. H., Bellwood D. R., Card M., Connolly S. R., Folke C., Grosberg R., Hoegh-Guldberg O., Jackson J. B. C., Kleypas J., Lough J. M., Marshall P. A., Nystrom M., Palumbi S. R., Pandolfi J. M., Rosen B. and Roughgarden J. (2003) Climate change, human impacts, and the resilience of coral reefs. *Science* **301**, 929–933.

Inoue M., Suzuki A., Nohara M., Kan H., Edward A. and Kawahata H. (2004) Coral skeletal tin and copper concentrations at Pohnpei, Micronesia: possible index for marine pollution by toxic anti-biofouling paints. *Environ. Pollut.* **129**, 399–407.

Johnson D. P. and Risk M. (1987) Fringing reef growth on a terrigenous mud foundation, Fantome Island, central Great Barrier Reef, Australia. *Sedimentology* **34**, 275–287.

Johnson J. E., Waterhouse J., Maynard J. A. and Morris S. (2010) *Reef Rescue Marine Monitoring Program: 2008/2009 Synthesis Report*. Reef and Rainforest Research Centre Limited, Cairns. p. 160.

Jompa J. and McCook L. J. (2003) Contrasting effects of turf algae on corals: massive *Porites* spp. are unaffected by mixed-species turfs, but killed by the red alga *Anotrichium tenue*. *Mar. Ecol.-Prog. Ser.* **258**, 79–86.

Knutson D. W., Buddemeier R. W. and Smith S. V. (1972) Coral chronometers: seasonal growth bands in reef corals. *Science* **177**, 270–272.

Larcombe P. and Woolfe K. J. (1999) Terrigenous sediments as influences upon Holocene nearshore coral reefs, central Great Barrier Reef, Australia. *Aust. J. Earth Sci.* **46**, 141–154.

Lea D. W., Shen G. T. and Boyle E. A. (1989) Coralline barium records temporal variability in equatorial pacific upwelling. *Nature* **340**, 373–375.

Lea D. W. and Boyle E. A. (1993) Determination of carbonate-bound barium in foraminifera and corals by isotope dilution plasma-mass spectrometry. *Chem. Geol.* **103**, 73–84.

Linsley B. K., Wellington G. M. and Schrag D. P. (2000) Decadal sea surface temperature variability in the subtropical South Pacific from 1726 to 1997 AD. *Science* **290**, 1145–1148.

Lough J. M. and Barnes D. J. (1990) Intra-annual timing of density band formation of *Porites* coral from the central Great Barrier Reef. *J. Exp. Mar. Biol. Ecol.* **135**, 35–57.

Ludwig K. R. (2003) Users Manual for Isoplot/Ex version 3.0: a Geochronological Toolkit for Microsoft Excel. Berkeley Geochronology Centre Special, Publication No. 3. Berkeley.

Mallela J., Hermann J., Rapp R. P. and Eggins S. M. (2011) Fine-scale phosphorus distribution in coral skeletons: combining X-ray mapping by electronprobe microanalysis and LA-ICP-MS. *Coral Reefs* **30**, 813–818.

Marshall P. A. and Baird A. H. (2000) Bleaching of corals on the Great Barrier Reef: differential susceptibilities among taxa. *Coral Reefs* **19**, 155–163.

Marshall J. F. and McCulloch M. T. (2002) An assessment of the Sr/Ca ratio in shallow water hermatypic coral as a proxy for sea surface temperature. *Geochim. Cosmochim. Acta* **66**, 3263–3280.

McClanahan T. R., Weil E. and Maina J. (2009) Strong relationship between coral bleaching and growth anomalies in massive *Porites*. *Global Change Biol.* **15**, 1804–1816.

McCulloch M. T., Fallon S. J., Wyndham T., Hendy E. J., Lough J. M. and Barnes D. J. (2003) Coral record of increased sediment flux to the inner Great Barrier Reef since European settlement. *Nature* **421**, 727–730.

McCulloch M. T., Gagan M. K., Mortimer G. E., Chivas A. R. and Isdale P. J. (1994) A high-resolution Sr/Ca and $\delta^{18}O$ coral record from the Great Barrier Reef, Australia, and the 1982–1983 El Niño. *Geochim. Cosmochim. Acta* **58**, 2747–2754.

McCulloch M. T. and Mortimer G. E. (2008) Applications of the ^{238}U–^{230}Th decay series to dating of fossils and modern corals using MC-ICP-MS. *Aust. J. Earth Sci.* **55**, 955–965.

McGregor H. V. and Gagan M. K. (2003) Diagenesis and geochemistry of *Porites* corals from Papua New Guinea: implications for paleoclimate reconstruction. *Geochim. Cosmochim. Acta* **67**, 2147–2156.

Meibom A., Stage M., Wooden J., Constantz B. R., Dunbar R. B., Owen A., Grumet N., Bacon C. R. and Chamberlain C. P. (2003) Monthly strontium/calcium oscillations in symbiotic coral aragonite: biological effects limiting the precision of the paleotemperature proxy. *Geophys. Res. Lett.* **30**, 1418. http://dx.doi.org/10.1029/2002GL016864.

Mitsuguchi T., Matsumoto E. and Uchida T. (2003) Mg/Ca and Sr/Ca ratios of *Porites* coral skeleton: evaluation of the effect of skeletal growth rate. *Coral Reefs* **22**, 381–388.

Mumby P. J., Chisholm J. R. M., Edwards A. J., Clark C. D., Roark E. B., Andrefouet S. and Jaubert J. (2001) Unprecedented bleaching-induced mortality in *Porites* spp. at Rangiroa Atoll, French Polynesia. *Mar. Biol.* **139**, 183–189.

Nothdurft L. D., Webb G. E., Bostrom T. and Rintoul L. (2007) Calcite-filled borings in the most recently deposited skeleton in live-collected *Porites* (Scleractinia): implications for trace element archives. *Geochim. Cosmochim. Acta* **71**, 5423–5438.

Nothdurft L. D. and Webb G. E. (2009a) Clypeotheca, a new skeletal structure in corals: a potential stress indicator. *Coral Reefs* **28**, 143–153.

Nothdurft L. D. and Webb G. E. (2009b) Earliest diagenesis in scleractinian coral skeletons: implications for palaeoclimate-sensitive geochemical archives. *Facies* **55**, 161–201.

Okai T., Suzuki A., Kawahata H., Terashima S. and Imai N. (2002) Preparation of a new Geological Survey of Japan

geochemical reference material: Coral JCp-1. *Geostandard. Newslett.* **26**, 95–99.

Pandolfi J. M., Bradbury R. H., Sala E., Hughes T. P., Bjorndal K. A., Cooke R. G., McArdle D., McClenachan L., Newman M. J. H., Paredes G., Warner R. R. and Jackson J. B. C. (2003) Global trajectories of the long-term decline of coral reef ecosystems. *Science* **301**, 955–958.

Pandolfi J. M., Connolly S. R., Marshall D. J. and Cohen A. L. (2011) Projecting coral reef futures under global warming and ocean acidification. *Science* **333**, 418–422.

Pandolfi J. M. and Greenstein B. J. (1997) Preservation of community structure in death assemblages of deep-water Caribbean reef corals. *Limnol. Oceanogr.* **42**, 1505–1516.

Quinn T. M. and Taylor F. W. (2006) SST artifacts in coral proxy records produced by early marine diagenesis in a modern coral from Rabaul, Papua New Guinea. *Geophys. Res. Lett.* **33**. http://dx.doi.org/10.1029/2005GL024972.

R Core Team (2013) R: A language and environment for statistical computing. R Foundation for Statistical Computing, Vienna, Austria.

Roff G. (2010) Historical ecology of coral communities from the inshore Great Barrier Reef. Ph. D. thesis. The University of Queensland, Brisbane.

Roff G., Clark T. R., Reymond C. E., Zhao J.-X., Feng Y.-X., McCook L. J., Done T. J. and Pandolfi J. M. (2013) Palaeoecological evidence of a historical collapse of corals at Pelorus Island, inshore Great Barrier Reef, following European settlement. *Proc. R. Soc. B: Biol. Sci.* **280**, 1750.

Rotjan R. D. and Lewis S. M. (2005) Selective predation by parrotfishes on the reef coral *Porites astreoides*. *Mar. Ecol.-Prog. Ser.* **305**, 193–201.

Scholz D. and Mangini A. (2007) How precise are U-series coral ages? *Geochim. Cosmochim. Acta* **71**, 1935–1948.

Shashar N., Banaszak A. T., Lesser M. P. and Amrami D. (1997) Coral endolithic algae: life in a protected environment. *Pac. Sci.* **51**, 167–173.

Shen C. C., Chiu H. Y., Chiang H. W., Chu M. F., Wei K. Y., Steinke S., Chen M. T., Lin Y. S. and Lo L. (2007) High precision measurements of Mg/Ca and Sr/Ca ratios in carbonates by cold plasma inductively coupled plasma quadrupole mass spectrometry. *Chem. Geol.* **236**, 339–349.

Shen C., Li K., Sieh K., Natawidjaja D. H., Cheng H., Wang X., Edwards R. L., Lam D. D., Hsieh Y., Fan T., Meltzner A. J., Taylor F. W., Quinn T. M., Chiang H. and Kilbourne K. H. (2008) Variation of initial $^{230}Th/^{232}Th$ and limits of high precision U–Th dating of shallow water corals. *Geochim. Cosmochim. Acta* **72**, 4201–4223.

Smithers S. G. and Woodroffe C. D. (2001) Coral microatolls and 20th century sea level in the eastern Indian Ocean. *Earth Planet. Sci. Lett.* **191**, 173–184.

Stirling C. H., Andersen M. B., Potter E. K. and Halliday A. N. (2007) Low-temperature isotopic fractionation of uranium. *Earth Planet. Sci. Lett.* **264**, 208–225.

Stirling C. H., Esat T. M., McCulloch M. T. and Lambeck K. (1995) High-precision U-series dating of corals from Western Australia and implications for the timing and duration of the Last Interglacial. *Earth Planet. Sci. Lett.* **135**, 115–130.

Suzuki A., Gagan M. K., Fabricius K., Isdale P. J., Yukino I. and Kawahata H. (2003) Skeletal isotope microprofiles of growth perturbations in Porites corals during the 1997–1998 mass bleaching event. *Coral Reefs* **22**, 357–369.

Sweatman H., Cheal A., Coleman G., Emslie M., Johns M., Jonker M., Miller I. and Osborne K. (2008) Long-term monitoring of the Great Barrier Reef: Status Report No. 8. Australian Institute of Marine Science, Townsville.

Sweatman H., Delean S. and Syms C. (2011) Assessing loss of coral cover on Australia's Great Barrier Reef over two decades, with implications for longer-term trends. *Coral Reefs* **30**, 521–531.

Thompson A. and Malcolm H. (1999) Benthic and fish monitoring of fringing reefs in the Brook, Palm and Rattlesnake Island groups: Status post 1998 coral bleaching event. Technical Report to the Queensland Parks and Wildlife Service.

Thompson A., Davidson J., Schaffelke B. and Sweatman H. (2010) Reef Rescue Marine Monitoring Program. Final Report of AIMS Activities – Inshore coral reef monitoring 2009/10. Australian Institute of Marine Science, Townsville.

Thompson A. A. and Dolman A. M. (2010) Coral bleaching: one disturbance too many for near-shore reefs of the Great Barrier Reef. *Coral Reefs* **29**, 637–648.

Tribollet A. and Golubic S. (2005) Cross-shelf differences in the pattern and pace of bioerosion of experimental carbonate substrates exposed for 3 years on the northern Great Barrier Reef, Australia. *Coral Reefs* **24**, 422–434.

van Woesik R. and Done T. J. (1997) Coral communities and reef growth in the southern Great Barrier Reef. *Coral Reefs* **16**, 103–115.

Vermeesch P. (2012) On the visualisation of detrital age distributions. *Chem. Geol.* **312–313**, 190–194.

Wakeford M., Done T. J. and Johnson C. R. (2008) Decadal trends in a coral community and evidence of changed disturbance regime. *Coral Reefs* **27**, 1–13.

Wesseling I., Uychiaoco A. J., Alino P. M., Aurin T. and Vermaat J. E. (1999) Damage and recovery of four Philippine corals from short-term sediment burial. *Mar. Ecol.-Prog. Ser.* **176**, 11–15.

Whelan K. R. T., Miller J., Sanchez O. and Patterson M. (2007) Impact of the 2005 coral bleaching event on *Porites porites* and *Colpophyllia natans* at Tektite Reef, US Virgin Islands. *Coral Reefs* **26**, 689–693.

Wilkinson C. (2008) Status of Coral Reefs of the World: 2008. Global Coral Reef Monitoring Network Reef and Rainforest Research Centre, Townsville, 304 pages.

Wooldridge S. A. and Done T. J. (2009) Improved water quality can ameliorate effects of climate change on corals. *Ecol. Appl.* **19**, 1492–1499.

Yu K.-F., Zhao J.-X., Lawrence M. G. and Feng Y. (2010) Timing and duration of growth hiatuses in mid Holocene massive *Porites* corals from the northern South China Sea. *J. Quatern. Sci.* **25**, 1284–1292.

Yu K.-F., Zhao J.-X., Liu T.-S., Wei G.-J., Wang P.-X. and Collerson K. D. (2004) High-frequency winter cooling and reef coral mortality during the Holocene climatic optimum. *Earth Planet. Sci. Lett.* **224**, 143–155.

Yu K.-F., Zhao J.-X., Roff G., Lybolt M., Feng Y.-X., Clark T. R. and Li S. (2012a) High-precision U-series ages of transported coral blocks on Heron Reef (southern Great Barrier Reef) and storm activity during the past century. *Palaeogeogr. Palaeocl.* **337–338**, 23–36.

Yu K.-F., Zhao J.-X., Shi Q., Chen T.-G., Wang P.-X., Collerson K. D. and Liu T.-S. (2006) U-series dating of dead *Porites* corals in the South China Sea: evidence for episodic coral mortality over the past two centuries. *Quat. Geochronol.* **1**, 129–141.

Yu K.-F., Zhao J.-X., Shi Q. and Price G. J. (2012b) Recent massive coral mortality events in the South China Sea: was global warming and ENSO variability responsible? *Chem. Geol.* **320–321**, 54–65.

Zhao J.-X., Hu K., Collerson K. D. and Xu H. K. (2001) Thermal ionisation mass spectrometry U-series dating of a hominid site near Nanjing, China. *Geology* **29**, 27–30.

Zhao J.-X., Yu K.-F. and Feng Y.-X. (2009) High-precision ^{238}U–^{234}U–^{230}Th disequilibrium dating of the recent past – a review. *Quat. Geochronol.* **4**, 423–433.

Zhou H. Y., Zhao J.-X., Wang Q., Feng Y.-X. and Tang J. (2011) Speleothem-derived Asian summer monsoon variations in Central China during 54–46 ka. *J. Quatern. Sci.* **26**, 781–790.

Associate editor: Claudine Stirling